

MATHEMATICAL MODELING FOR ADIABATIC FLOW OF REFRIGERANT IN HELICAL CAPILLARY TUBE

A thesis submitted in partial fulfillment of the requirements for the award of

degree of

MASTER OF ENGINEERING

IN

THERMAL ENGINEERING

Submitted By:

AMANDEEP SINGH

Roll No: 801083001

Under the guidance of:

Dr. MADHUP KUMAR MITTAL

Assistant Professor, Deptt. of Mechanical Engg.

Thapar University, Patiala



DEPARTMENT OF MECHANICAL ENGINEERING

THAPAR UNIVERSITY

PATIALA – 147004

JULY, 2012


DECLARATION

I hereby declare that work in this thesis entitled, “**Mathematical modeling for adiabatic flow of refrigerant in helical capillary tube**”, in partial fulfillment of the requirements for the award of degree of Master of Engineering in mechanical engineering with specialization in **THERMAL ENGINEERING** submitted in Mechanical Engineering Department of Thapar University, Patiala, is an authentic record of my own work carried out under the supervision Dr. Madhup Kumar Mittal.


The matter presented in this thesis has not been submitted for the award of any other degree of this or any other university.

Date: 13-07-2012

Place: PATIALA


(AMANDEEP SINGH)

This is to certify that the above statement made by candidate is correct and true to the best of my knowledge.

Supervisor 
Dr. Madhup Kumar Mittal
Assistant Professor, MED
Thapar University, Patiala

ACKNOWLEDGEMENT

I express my sincere gratitude to **Dr. Madhup Kumar Mittal, Assistant Professor, Mechanical Engineering Department, Thapar University, Patiala**, for their valuable guidance, proper advice and constant encouragement of my work in this thesis.

I do not find enough words with which I can express my feeling of thanks to the entire faculty and staff of **Mechanical Engineering Department Thapar University, Patiala**, for their help, inspiration and moral support.




AMANDEEP SINGH

CERTIFICATE

This is to certify that the thesis report entitled, '**Mathematical modeling for adiabatic flow of refrigerant in helical capillary tube**', which is submitted by Amandeep Singh (801083001), in the partial fulfillment of the requirement for the award of Master of Engineering in Thermal Engineering from MED, Thapar University, Patiala, is a record of candidate's own work carried out by him under my supervision. The matter embodied in this thesis report is original and has not been submitted for the award of any other degree.


(Dr. Madhup Kumar Mittal)
Assistant Professor
Mechanical Engineering Department
Thapar University, Patiala



(Dr. Ajay Batish)
Professor and Head,
Mechanical Engineering Department
Thapar University, Patiala

(Counter Signed by)


(Dr. S.K. Mohapatra)
Dean of Academic Affairs,
Thapar University, Patiala

CONTENTS

Topic	Page No.
CHAPTER-I INTRODUCTION	1
1.1 Classification of refrigerant expansion devices	2
1.1.1 Capillary Tube	2
1.1.2 Hand operated expansion valve	2
1.1.3 Orifice	2
1.1.4 Constant pressure or automatic expansion valve (AEV)	2
1.1.5 Thermostatic expansion valve (TEV)	2
1.1.6 Float type expansion valve	2
1.1.7 Electronic expansion device	2
1.2 Environmental Concerns	4
1.3 Motivation for present study	5
1.4 Objective of present study	6
1.5 Organization of thesis	
CHAPTER- II LITERATURE REVIEW	9
2.1 Review of experimental work	11
2.2 Review of numerical work	15
2.3 Types of mathematical models	19
2.3.1 Homogeneous Flow Model	19
2.3.2 Separate Flow Model	19

2.3.3	Drift Flux Model	19
2.4	Conclusion from literature review	20
CHAPTER- III MATHEMATICAL MODEL		21
3.1	Formulation of mathematical model	21
3.1.1	Single phase region	24
3.1.2	Two phase region	26
CHAPTER- IV RESULTS AND DISCUSSION		31
4.1	Validation of mathematical model	
4.1.1	Validation of mathematical model with Mittal <i>et al.</i> (2009) experimental data for R-407 C with coil diameter 60 mm.	31
4.1.2	Validation of mathematical model with Mittal <i>et al.</i> (2009) experimental data for R-407 C with coil diameter 100 mm.	32
4.1.3	Validation of mathematical model with Mittal <i>et al.</i> (2009) experimental data for R-407 C with coil diameter 140 mm.	33
4.1.4	Validation of mathematical model with Mittal <i>et al.</i> (2009) experimental data for R-407 C with tube diameter 1.27 and coil diameter 60,100,140 mm.	34
4.1.5	Validation of mathematical model with Mittal <i>et al.</i> (2009) experimental data for R-407 C with tube diameter 1.27 and coil diameter 60,100,140 mm.	36
4.1.6	Validation of mathematical model with Kim <i>et al.</i> (2002) experimental data for R-407 C with coil diameter 40,120,200 mm.	38
4.1.7	Validation of mathematical model with Kim <i>et al.</i> (2002) experimental data for R-410 A with coil diameter 40,120,200 mm.	40
4.1.8	Validation of mathematical model with Khan <i>et al.</i> (2008) experimental data for R-134a with coil diameter 40,120,200 mm.	42
4.1.9	Validation of mathematical model with Khan <i>et al.</i> (2008) experimental data for R-134a with coil diameter 40,120,200 mm.	44

4.2 Simulation of refrigerants R-407 C, R-410 A, R134a, R-12 and R-404 A using M&N equation for both single and two phase length.	50
4.2.1 Simulation results of refrigerants R-407 C, R-410 A, R134a, R-12 and R-404 A using M&N equation for effect of sub cooling on mass flow rate.	51
4.2.2 Simulation results of refrigerants R-407 C, R-410 A, R134a, R-12 and R-404 A using M&N equation for effect of coil diameter on mass flow rate.	53
4.2.3 Simulation results of refrigerants R-407 C, R-410 A, R134a, R-12 and R-404 A using M&N equation for effect of evaporator pressure on mass flow rate.	55
4.2.4 Simulation results of refrigerants R-407 C, R-410 A, R134a, R-12 and R-404 A using M&N equation for effect of capillary tube diameter on mass flow rate.	57
4.2.5 Simulation results of refrigerants R-407 C, R-410 A, R134a, R-12 and R-404 A using M&N equation for effect of capillary tube inlet pressure on mass flow rate.	59
4.2.6 Variation of pressure of refrigerants R-407 C, R-410 A, R134a, R-12 and R-404 A along a capillary tube length.	60
4.2.7 Variation of temperature of refrigerants R-407 C, R-410 A, R134a, R-12 and R-404 A along a capillary tube length.	61
4.2.8 Different pressures of refrigerants R-407 C, R-410 A, R134a, R-12 and R-404 A along a capillary tube length.	62
4.2.9 Different temperature of refrigerants R-407 C, R-410 A, R134a, R-12 and R-404 A along a capillary tube length.	63

CHAPTER- V CONCLUSION AND SCOPE OF WORK

5.1 Conclusion	65
5.2 Scope of future work	66
Reference	67

LIST OF FIGURES

Sr. no	Description	Page No.
1.1	Typical single stage refrigeration system.	1
1.2	Pictorial diagram of a detachable capillary tube.	3
1.3	Systematic diagram of automatic expansion valve.	3
1.4	Systematic diagram of thermostatic expansion valve.	4
2.1	Helical and spiral capillary tube.	10
2.2	Secondary flow.	11
2.3	Computational domain capillary tube.	17
2.4	Force acting on a fluid element.	17
3.1	Systematic diagram of adiabatic helical capillary tube.	22
3.2	Free body diagram of fluid element of adiabatic helical capillary tube.	23
3.3	Systematic fluid element considerations in two phase flow in adiabatic helical capillary tube.	26
4.1	Comparison of Mittal <i>et al.</i> (2009) experimental data with present numerical results at condenser pressure of 16.4 bar for the flow of R-407 C with coil diameter 60 mm.	32
4.2	Comparison of Mittal <i>et al.</i> (2009) experimental data with present numerical results at condenser pressure of 16.4 bar for the flow of R-407 C with coil diameter 100 mm.	33
4.3	Comparison of Mittal <i>et al.</i> (2009) experimental data with present numerical results at condenser pressure of 16.4 bar for the flow of R-407 C with coil diameter 140 mm.	34
4.4, 4.5	Comparison of Mittal <i>et al.</i> (2009) experimental data with present numerical results at condenser pressure of 18.6 bar for the flow of R-407 C with coil diameter 60 mm and 100 mm.	35

4.6	Comparison of Mittal <i>et al.</i> (2009) experimental data with present numerical results at condenser pressure of 18.6 bar for the flow of R-407 C with coil diameter 140 mm.	36
4.7,4.8	Comparison of Mittal <i>et al.</i> (2009) experimental data with present numerical results at condenser pressure of 14.7 bar for the flow of R-407 C with coil diameter 60 mm and 100 mm .	37
4.9	Comparison of Mittal <i>et al.</i> (2009) experimental data with present numerical results at condenser pressure of 14.7 bar for the flow of R-407 C with coil diameter 140 mm.	38
4.10,4.11	Comparison of Kim <i>et al.</i> (2002) experimental data with present numerical results at condenser pressure of 19.72 bar for the flow of R-407 C with coil diameter 40 mm and 120 mm .	39
4.12	Comparison of Kim <i>et al.</i> (2002) experimental data with present numerical results at condenser pressure of 19.72 bar for the flow of R-407 C with coil diameter 200 mm.	40
4.13,4.14	Comparison of Kim <i>et al.</i> (2002) experimental data with present numerical result at condenser pressure of 27.33 bar for the flow of R-410 A with coil diameter 40 mm and 120 mm.	41
4.15	Comparison of Kim <i>et al.</i> (2002) experimental data with present numerical results at condenser pressure of 27.33 bar for the flow of R-410 A with coil diameter 200 mm.	42
4.16,4.17	Comparison of Khan <i>et al.</i> (2008) experimental data with present numerical result at condenser pressure of 7.23 bar for the flow of R-134a with coil diameter 140 mm.	43
4.18	Comparison of Khan <i>et al.</i> (2008) experimental data with present numerical results at condenser pressure of 7.23 bar for the flow of R-134a with coil diameter 140 mm.	44
4.19,4.20	Comparison of Khan <i>et al.</i> (2008) experimental data with present numerical results at condenser pressure of 7.23 bar for the flow of R-134a with coil diameter 140 mm.	45

4.21	Comparison of Khan <i>et al.</i> (2008) experimental data with present numerical results at condenser pressure of 7.23 bar for the flow of R-134a with coil diameter 140 mm.	46
4.22,4.23	Comparison of measured mass flow rate and predicted mass flow rate deviation of refrigerant R407 C and R 410 A using M&N, M&N+GIRI and C-M&N equations.	47
4.24	Comparison of measured mass flow rate and predicted mass flow rate deviation of refrigerant R 134a using M&N, M&N+GIRI and C-M&N equations.	48
4.25 (a, b)	Comparison of measured mass flow rate with predicted mass flow rate for refrigerants R-134a and R-407 C.	49
4.25 (c)	Comparison of measured mass flow rate with predicted mass flow rate for refrigerants R-134a and R-407 C.	50
4.26	Mass flow rate variation with degree of sub cooling for refrigerants R-407 C, R-410 A, R134a, R-12 and R-404 A for lengths of 2 m and 1.27 mm tube diameter and condenser temperature of 42.5°C.	51
4.27,4.28	Mass flow rate variation with degree of sub cooling for refrigerants R-407 C, R-410 A, R134a, R-12 and R-404 A for lengths of 1, 2 m and 1.27,1.02 mm tube diameter and condenser temperature of 45and37.38 °C.	52
4.29	Mass flow rate variation with coil diameter for refrigerants R-407 C, R-410 A, R134a, R-12 and R-404 A for lengths of 2 m and 1.27 mm tube diameter, sub cooling 3°C and condenser temperature of 42.5°C.	53
4.30,4.31	Mass flow rate variation with coil diameter for refrigerants R-407 C, R-410 A, R134a, R-12 and R-404 A for lengths of 2 m and 1.27 mm tube diameter, sub cooling 6,9°C, and condenser temperature of 42.5°C.	54
4.32	Mass flow rate variation with evaporator pressure for refrigerants R-407 C, R-410 A, R134a, R-12 and R-404 A for lengths of 2 m and 1.5 mm tube diameter, sub cooling 3°C and condenser temperature of 45°C.	55

4.33,4.34	Mass flow rate variation with evaporator pressure for refrigerants R-407 C, R-410 A, R134a, R-12 and R-404 A for lengths of 2 m and 1.5,1 mm tube diameter, sub cooling 6°C and condenser temperature of 45,35°C.	56
4.35	Mass flow rate variation with evaporator pressure for refrigerants R-407 C, R-410 A, R134a, R-12 and R-404 A for lengths of 2 m and 1 mm tube diameter, sub cooling 10°C and condenser temperature of 35°C.	57
4.36,4.37	Mass flow rate variation with capillary tube diameter for refrigerants R-407 C, R-410 A, R134a, R-12 and R-404 A for lengths of 1,2 m, coil diameter 80,100 mm, sub cooling 3°C and condenser temperature of 38 and 42°C.	58
4.38	Mass flow rate variation with inlet pressure for refrigerants R-407 C, R-410 A, R134a, R-12 and R-404 A for lengths of 1 m and 1.3 mm tube diameter, sub cooling 3°C and coil diameter 120 mm.	59
4.39	Mass flow rate variation with inlet pressure for refrigerants R-407 C, R-410 A, R134a, R-12 and R-404 A for lengths of 2 m and 1.6 mm tube diameter, sub cooling 6°C and coil diameter 140 mm.	60
4.40	Variation of pressure for refrigerants R-407 C, R-410 A, R134a, R-12 and R-404 A along a capillary tube length for pressure 22 bar, 1.15 mm tube diameter, sub cooling 5°C and coil diameter 60 mm.	61
4.41	Variation of temperature for refrigerants R-407 C, R-410 A, R134a, R-12 and R-404 A along a capillary tube length for temperature 42°C, 1.7 mm tube diameter, sub cooling 5°C and coil diameter 110 mm.	62
4.42	Different pressure variation for refrigerants R-407 C, R-410 A, R134a, R-12 and R-404 A along a capillary tube length for saturation temperature 42°C, 1.7 mm tube diameter, sub cooling 5°C and coil diameter 110 mm.	63
4.43	Different pressure variation for refrigerants R-407 C, R-410 A, R134a, R-12 and R-404 A along a capillary tube length for saturation pressure 22 bar, 1.15 mm tube diameter, sub cooling 5°C and coil diameter 60 mm.	64

LIST OF TABLES

3.1	Different study values.	25
3.2	Two phase viscosity co relation models	29
4.1	Details for experimental data of adiabatic helical capillary tube to validate the model.	31

NOMENCLATURE

A	cross-sectional area of capillary tube (m^2)
d_i	diameter of capillary tube (m)
D_c	coil diameter (m)
De	dean number
f	friction factor
g	gravitational acceleration (m/s^2)
G	mass flow rate per unit area (kg/s m^2)
h	specific enthalpy
k	entrance loss coefficient
L	length of capillary tube (m)
m	mass flow rate (kg/s)
p	pitch of coil (m)
P	pressure (Pa)
Re	Reynolds number
s	specific entropy (j/kg K)
ΔT_{sub}	degree of sub cooling ($^{\circ}\text{C}$)
T	temperature ($^{\circ}\text{C}$)
V	velocity (m/s)
x	quality
Z	elevation head

Greek letters

τ	wall shear stress (N/m^2)
v	specific volume (m^3/kg)
μ	dynamic viscosity (kg/m s)
ρ	density (kg/m^3)
ε	surface roughness (m)

Subscripts

evap evaporator

f,g liquid phase and gas phase

i capillary inlet

sp,tp single phase and two phase, respectively

w wall

crit critical

ABSTRACT

Present work has been carried out to investigate the flow characteristics of refrigerants R-407 C, R-134a, R-410 A, R-12 and R-404 A flowing through helical capillary tube under adiabatic flow conditions. The parametric study was conducted by varying operating conditions and geometrical parameters of the capillary tube. A mathematical model has been developed to predict the performance of a refrigerant in helical capillary tube under adiabatic flow conditions. The proposed model can predict the length of the adiabatic helical capillary tube for a given mass flow rate or the mass flow rate through a given length of capillary tube. A computer program coded in MATLAB has been developed to compute either length or mass flow rate by fixing some of parameter. This model also includes the effect of various design parameters, like capillary tube diameter, capillary tube coil diameter, degree of sub-cooling, evaporator pressure, inlet pressure, mass flow rate. Thermodynamic and transport property can derived from advanced property data base such as REFPROP. The mathematical model based on homogenous two phase flow without considering metastable length has been developed to predict the flow characteristics of a refrigerant in helical capillary tube for adiabatic flow conditions. A set of differential equations is obtained by applying the law of conservation of mass, momentum and energy. These differential equations are solved using finite difference method. Different correlations for friction factor and viscosity available in the literature are used in the model. Performance of conventional and non conventional refrigerants can be compared under different operating conditions. The developed model can be considered as an effective tool for designing and optimizing capillary tubes working with newer alternative refrigerants. The model is validated by comparison with the experimental data of Kim *et al.* (2002) for R-22, R-407C and R-410A, Zhou and Zhang (2006) for R-22 and Khan *et al* (2009) for R-134a. The results obtained from the present model show reasonable agreement with the experimental data. The proposed model can be used to design helical capillary tubes working with various refrigerants.

Chapter I

INTRODUCTION

Fig. 1.1 shows the single stage vapor compression refrigeration system in its simplest form. The throttling of refrigerant from high pressure side to low pressure side of an air conditioner/heat pump may be accomplished by a variety of devices, the most common being the thermostatic expansion valves, capillary tubes and the plug orifices. A capillary tube is a constant area expansion device, which is commonly used in small refrigeration and air-conditioning systems. It is a simple tube with inner diameters of a few millimeters, but the flow inside a capillary tube is very complex and pressure drop through the capillary tube has a strong influence on the performance of the whole system. It has advantages of simplicity, inexpensiveness, and the requirement of low starting torque of a compressor. However, reduction in cycle efficiency when load condition changes, is one of the major disadvantages in adopting a capillary tube as an expansion device because the capillary tube does not have any function to actively adjust to this change.

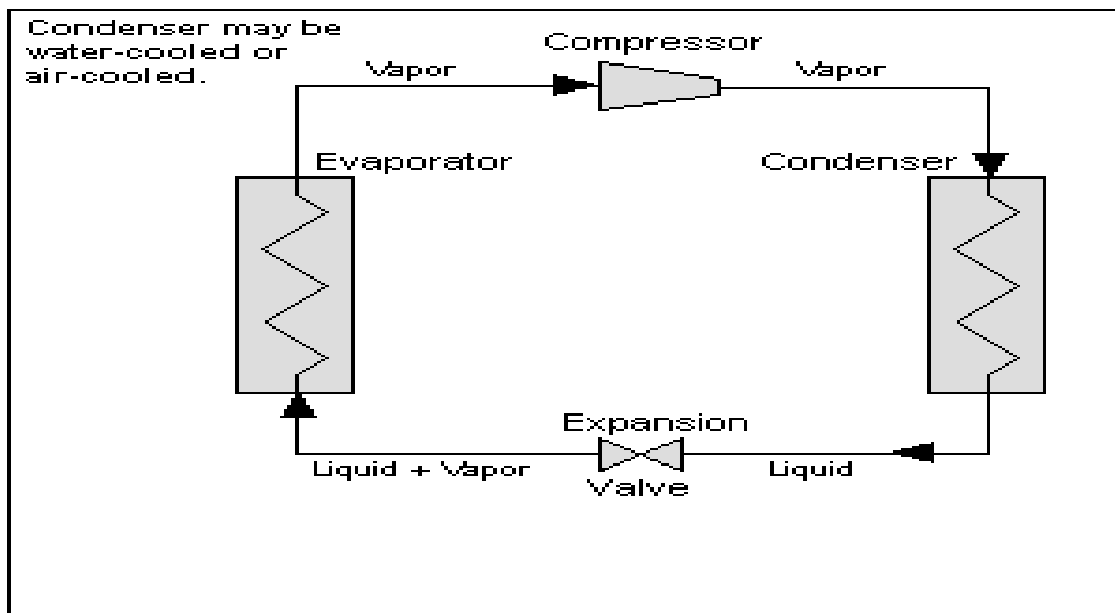


Figure 1.1 Typical single stage refrigeration system

The capillary tube dimensions play a vital role in deciding its contribution to performance of the refrigeration system. The shape of the coiled capillary tube can considerably affect the mass flow

rate in the refrigeration cycle because the flow resistance from the secondary flow varies with the coiled shape. Since an improperly sized capillary tube can significantly reduce the performance of a refrigeration system, an appropriate tool for the optimal design of the coiled capillary tube is essential. Although there have been many studies on the flow characteristics and modeling of straight capillary tubes, studies on the spirally coiled capillary tube have been very limited. Practical redesign of the system by adopting a different capillary tube for alternative refrigerant requires the determination of the length and the diameter of capillary tube for a given refrigeration on capacity and operating conditions.

1.1 Classification of refrigerant expansion devices

Expansion devices can be classified:

1.1.1 Capillary tube

Straight capillary tube

- (a) Adiabatic capillary tube
- (b) Diabatic capillary tube

Coiled capillary tube

- (a) Helical capillary tube
- (b) Spiral capillary tube

1.1.2 Hand operated expansion valves

1.1.3 Orifice

1.1.4 Constant pressure or automatic expansion devices (AEV)

1.1.5 Thermostatic expansion valve (TEV)

1.1.6 Float type expansion valve

1.1.7 Electronic expansion valve

Of the above seven types, Capillary tube and orifice belong to the fixed opening type, while the rest belong to the variable opening type. Of the above seven types, the hand operated expansion valve is not used when an automatic control is required. The orifice type expansion is used only



Figure 1.2 Pictorial diagram of a detachable capillary tube

in some special applications. An Automatic Expansion Valve (Fig 1.3) also known as a constant pressure expansion valve acts in such a manner so as to maintain a constant pressure and thereby a constant temperature in the evaporator. The automatic expansion valves are used wherever constant temperature is required for milk chilling units and water coolers where freezing is disastrous.

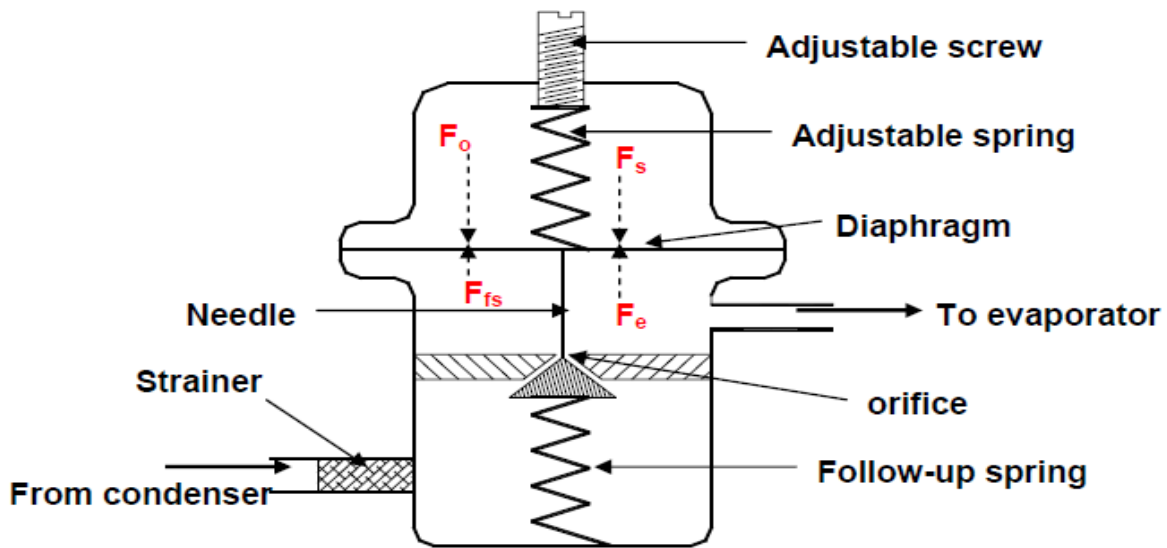


Figure 1.3 Systematic diagram of automatic expansion valve

Thermostatic expansion (Fig 1.4) valve is the most versatile expansion valve and is most commonly used in refrigeration systems. A thermostatic expansion valve maintains a constant degree of superheat at the exit of evaporator; hence it is most effective for dry evaporators in preventing the slugging of the compressors since it does not allow the liquid refrigerant to enter the compressor.

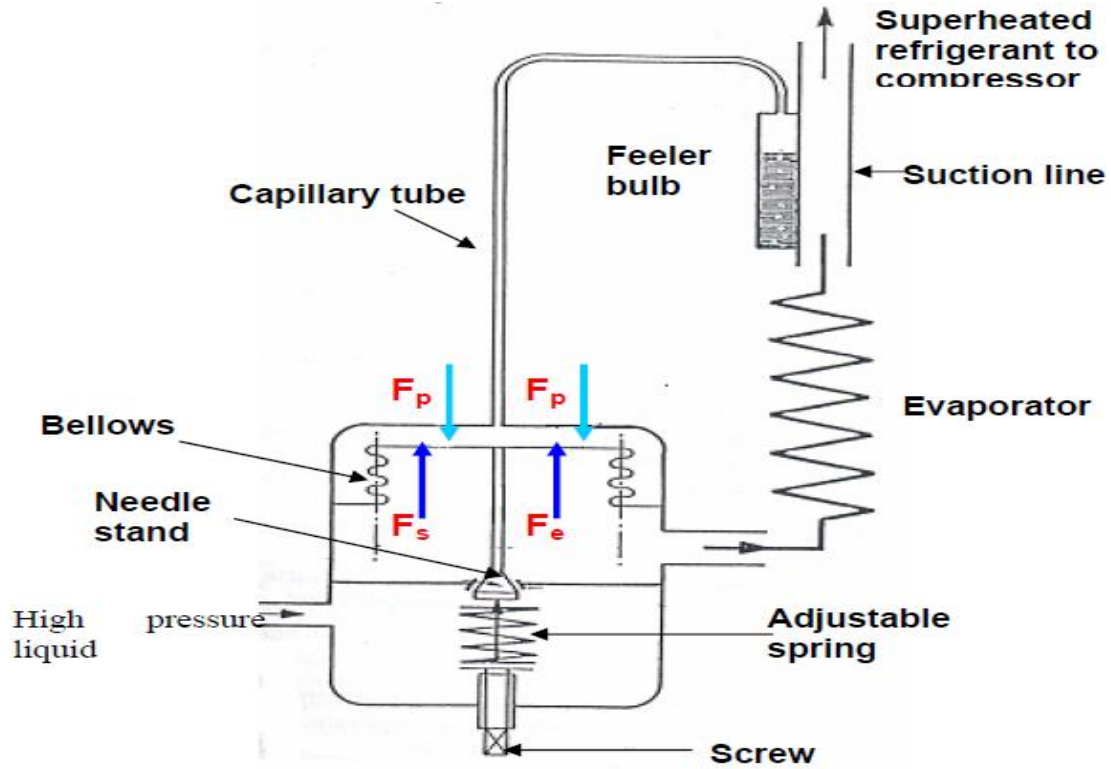


Figure 1.4 Systematic diagram of thermostatic expansion valve

1.2 Environmental concerns

Due to environmental concerns on the depletion of ozone layer and global warming, CFC (chlorofluorocarbon) and HCFC (hydro chlorofluorocarbon) are being phased out from refrigeration industry. As a result HFC (hydro fluorocarbon), HC (hydrocarbon) and HFC mixtures have emerged as an alternative to R-12 and R-22. In fact, the earth is enveloped in a thin shell of ozone layer which prevents the earth from harmful ultra-violet radiations coming from the sun. The chlorine present in conventional refrigerants is responsible for the depletion of the protective layer of ozone in the upper atmosphere. This leads to increased level of ultraviolet radiation reaching the earth's surface, which result in higher rates of skin cancer, eye cataracts

and damage to people's immune system. As the free molecule of conventional refrigerant reaches the upper atmosphere, the strong solar radiations break down the conventional refrigerant's molecule freeing chlorine atom from the structure. This chlorine reacts with ozone and converts it to oxygen. The conversion of ozone into oxygen will ultimately cause thinning of the layer to the extent that a hole is formed. This depleted zone of the ozone layer is termed as 'Ozone Hole'.

The conventional refrigerants have varying degree of ozone depletion potential (ODP). In the lower atmosphere, the molecules of conventional refrigerants absorb Infrared radiations, which may contribute the warming of the earth, i.e., conventional refrigerants also act as greenhouse gases and, thus, have a global warming potential (GWP). The extent to which a greenhouse gas contributes to global warming depends on the amount of it that is emitted, the length of time which elapses before it is purged from the atmosphere and the infrared energy absorption properties of the gas. Thus global warming from a greenhouse gas is connected to a particular time scale (e.g., 100 or 500 years) known as integrated time horizon (ITH). For regulatory purposes, the convention is to use the 100-year integrated time horizon. The Global Warming Potential (GWP) of a greenhouse gas is the ratio of global warming caused from one unit mass of a greenhouse gas to that of one unit mass of carbon dioxide over a period of time. Nowadays, the unusual rise in global temperatures or global warming is mainly because of the rapid industrialization which has guided the way to the production of several green house gases and CO₂ in particular.

1.3 Motivation for the present study

As conventional refrigerants are being phased-out, newer environmentally safe refrigerants are coming to market. R-407C, R-404 and R-410 A are such refrigerants, which has thermo physical properties closer to those of R-22 and it is a potential replacement of R-22 as it is environmentally safe. For air conditioning applications the best choice available in the market is R-410 A and for refrigeration best choice is R-404 A and R-507. On the other hand only replacement available of R-12 is R134a. R-134a only approved vehicle refrigerant currently approved by all vehicle manufacturers for retrofitting older R-12 A/C system. When alternative refrigerants are applied to air conditioning and refrigeration system, each component of the system must be redesigned to achieve a higher reliability and performance of system. The study

on capillary tube, which is one of the important components of refrigeration system, is of much importance as an improperly sized capillary tube significantly reduces the performance of refrigeration system.

Mathematical modeling is also one of the methods to size a capillary tube for different operating conditions of a refrigeration system. Thus, to simulate the performance of an adiabatic helical capillary tube, mathematical models for adiabatic flow arrangement have been developed for different helical capillary tube geometries. A number of friction factor and viscosity correlation are available in the literature. In the proposed work a suitable combination of friction factor and viscosity model has been taken for sizing the helical capillary tube design parameters.

1.4 Objective of the present work

The objective of the present study is to develop a mathematical flow model to analyze the flow characteristics of refrigerant flowing through the adiabatic helical capillary tube.

1. Development of mathematical model for the flow of refrigerant through adiabatic helical capillary tube.
2. The aim of the present work is to compare the flow performance of conventional and non conventional refrigerants.
3. To simulate the performance of capillary tube, mathematical model for adiabatic flow arrangement is to be developed for adiabatic helical capillary tube.

1.5 Organization of thesis

The thesis has been divided mainly into five parts. The mathematical model and validation of simulated results with experimental results has been presented in the thesis. Moreover predictions of mass flow rate for non conventional refrigerants for various geometries are also carried out in the presented work.

Chapter I

This chapter is related to the capillary tube introduction and introductory phrase of single stage refrigeration system. This chapter is about dimensions and complexity of refrigerant flow in a capillary tube. The classification of the capillary tubes and brief working of some type of capillary tubes are described. It presents the advantage and disadvantage and environmental concerns. Motivation for the present study and objectives are also described in this chapter.

Chapter II

It is related to literature review and problem formulation. Extensive literature on experimental work and numerical model available for straight and helical adiabatic capillary tube are reviewed. Categorization of capillary tube and secondary flow phenomenon presented in this chapter. In addition types of mathematical model and conclusion from literature review are also described.

Chapter III

This chapter is about formulation of mathematical model. It is related to the calculation of the length of the helical adiabatic capillary tube. It also describes the friction factor and viscosity model used in present mathematical model. This chapter is about the total length calculation of adiabatic capillary tube.

Chapter IV

This chapter deals with result and discussion. All the validation and simulation results plotted and discussed in this chapter. It includes Graphs for different geometries and inlet conditions. This chapter presents all the results obtained from the mathematical model.

Chapter V

This chapter includes the conclusion of the thesis. Various effects of different parameters on mass flow rate of refrigerant are discussed in this chapter.

Chapter - II

LITERATURE REVIEW

Review of the published literature on capillary tube expansion device used in refrigeration applications. In spite of simple configuration of capillary tube, the flow behavior of refrigerant in capillary tube is a complex phenomenon and the behavior of capillary tube is crucial to the performance of the refrigeration system, hence, a large number of experimental and numerical studies had been conducted in the past to understand the flow characteristics of refrigerant in a capillary tube.

The coiled tubes have been used as one of the passive heat transfer enhancement techniques due to their high heat transfer coefficient and they are widely used in various industrial applications due to their compact structure. Helical and spiral tubes are well known type of coiled tubes which have been used in a wide variety of applications, for example heat recovery processes, air conditioning and refrigeration systems, chemical reactors food and dairy processes. The capillary tubes are usually helically coiled in a domestic refrigerator or in a window air conditioner to save the space and to make a compact refrigeration system. However, the use of spiral capillary tube in a refrigeration system may still be considered a unique approach. The difference in the two geometries lies in the radius of curvature. In spiral capillary tubes, the radius of curvature varies continuously, whereas, it is constant in case of helical tubes. The difference between the consecutive turns of the coiled capillary tube is termed as coil pitch, denoted by ' p '. Another difference in the two geometries is that in spiral capillary tubes there is only one coiling parameter, i.e., coil pitch, whereas, in helical capillary tubes there are two coiling parameters one is coil pitch and another is coil diameter as shown in figure 2.1. The shape of the coiled capillary tube can considerably affect the mass flow rate in the refrigeration cycle because the flow resistance from the secondary flow varies with the coiled shape. Since an improperly sized capillary tube can significantly reduce the performance of a refrigeration system *Choi J.M and, Kim Y.C. (2002)*, an appropriate tool for the optimal design of the coiled capillary tube is essential. Although there have been many studies on the flow characteristics and modeling of straight capillary tubes, studies on the spirally coiled capillary tube have been very limited.

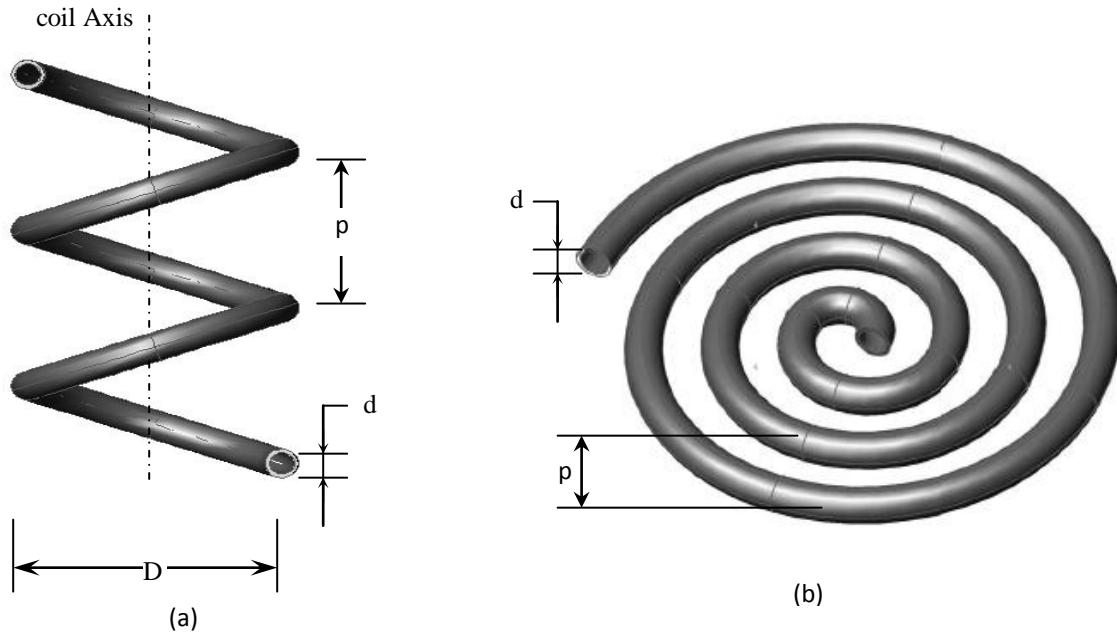


Figure 2.1 (a) helical capillary (b) spiral capillary

Capillary tube models can be classified into two categories, which are a numerical model and an empirical correlation. The determination of the friction factor in the capillary tube was the major part of the numerical modeling. Most theoretical models modified the friction factor based on measured data. The frictional pressure drop of a single-phase fluid flow through a curved tube is larger than that for a flow through a straight tube under similar conditions. The pressure drop of a coiled tube increased because of the secondary flow generated by a centrifugal force as shown in figure 2.2(a and b). The friction factor as a function of the dimensionless parameter is given by $Re \sqrt{\frac{d}{D}}$ which is known as Dean Number. The existence of secondary flow is called the Dean effect. The critical Reynolds number increases with the increase in ratio, d/D , and is expressed by the following relation proposed by *Ito.H (1959)*.

$$Re_{crit} = 20000 \left(\frac{d}{D_c} \right)^{0.32} \quad (2.1)$$

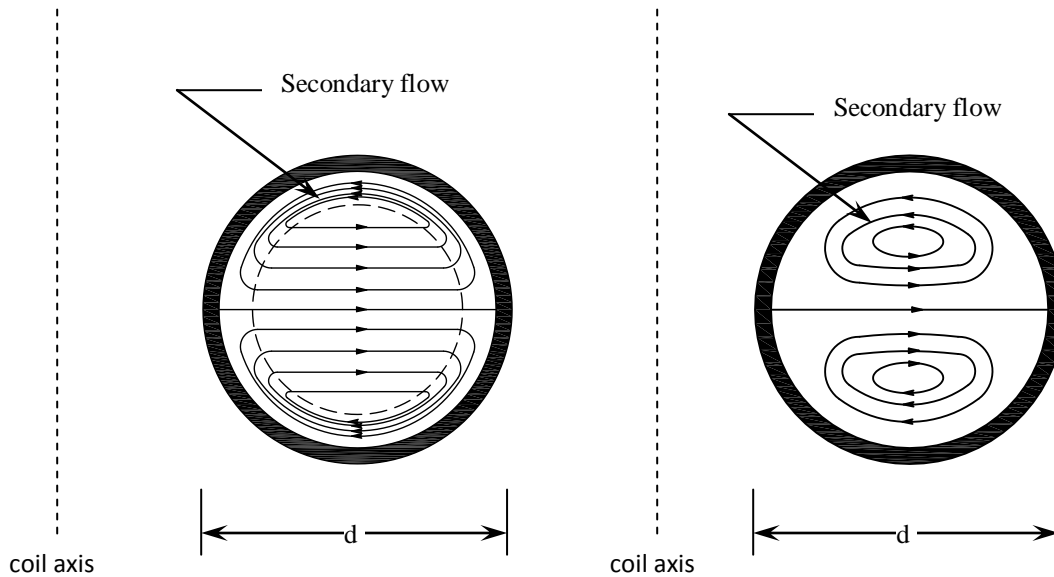


Figure 2.2 Secondary flow (a) large De (b) small De

2.1 Review of experimental work

It has been observed from the literature that most of the work either it is in form of experimental correlation or in form of numerical modeling is carried out on flow of refrigerant through straight capillary tube. First of all Kuehl S.J and Goldschmidt V.W (1990) set an experimental test set up and several capillary length and diameter combinations were tested. They were used a test loop that provided control of the sub cooling, and condenser and evaporator pressures. Tests were also performed to measure the distribution pressure drops and to determine the effect of coiling on the restriction characteristics of the capillary tube. Before them some investigators have argued that coiling has no effect upon the capillary tube performance, contending that the ratio of capillary tube diameter to radius of curvature is negligible. To determine if coiling indeed does not affect capillary tube performance, five capillary tubes with different diameters were used by them using the closed loop system. And the net result was that coiling, regardless of the percentage of the overall length coiled or the phase of refrigerant tends to increase the restriction characteristics of the capillary tube by approximately 5%. In their study they also did some work relative to the capillary tube relative roughness. But the results were somewhat discouraging in that test data for the different capillary bores did not follow along the lines of constant relative roughness in the steady diagrams; instead some of the data cross over the relative roughness levels.

Wei *et al.* (2000) proposed a performance comparison between straight and coiled capillary tube. As in Kuehl S.J and Goldschmidt V.W (1990) work they did not report any quantitative

relation about the effect of coiling, nor did they report the effect of inlet conditions (sub cooling and pressure) in conjunction with the effect of coiling. So Wei *et al.* (2000) worked to examine the difference between coiled capillary and straight capillary tubes quantitatively, and to investigate the inlet conditions in connection with the effect of coiling by using refrigerant R-22. In their work Thermodynamic and transport properties of the refrigerants were evaluated using the computer program REFPROP. Their test results indicated that the helical effect increased with decrease of coiling diameter and the effect of inlet sub cooling is insensitive to change of inlet pressure and sub cooling. Based on their test results, a correlation was proposed which can quantitatively describe the difference between coiled and straight capillary tubes.

$$\frac{m_{coiled}}{m_{straight}} = 2.011 \left(\frac{D_c}{L} \right)^{.0527} \left(\frac{d_i}{L} \right)^{.094} \quad (2.2)$$

Kim *et al.* (2002) presented their test results and developed a dimensionless correlation on the basis of experimental data of adiabatic capillary tube for R 22 and its alternatives. The performances of the adiabatic capillary tubes with several length and inner diameter combinations for R22 and its alternatives, R407C and R410A were experimentally investigated. The mass flow rates of R407C were greater by 4.0%, and those of R410A are greater by 23% as an average, than those of R22. The mass flow rates in capillary tubes with coiled diameter of 40 mm are approximately 9% less than those of straight capillary tubes. They agreed to the point that pressure drop of a coiled tube was increased due to existence of a secondary flow generated by a centrifugal forces as the case of common coiled pipes and thus the reduced mass flow rates. Dimensionless correlation was developed to predict mass flow rates through adiabatic capillary tubes as a function of several dimensionless parameters based on the Buckingham Ω theorem. The deviation of experimental results for R22, R407C and R410A from the dimensionless correlation in this study lies between -12% and +12% for all test conditions.

Guobing.Z and Yufeng.Z (2006) presented their numerical and experimental investigation on the performance of coiled adiabatic capillary tube. They developed four flow region model including metastable both liquid and two phase regions. They attempted to discuss the appropriate friction factor equations used in their flow model, which predict the mass flow rates in coiled capillary tubes. They were used three methods for calculating the friction factors of

refrigerant flow through capillary tubes. First is M&N + Giri method for liquid region, secondly M&N method for both liquid and two phase region and C-M&N method for both liquid and two phase region. The performance of straight and coiled adiabatic capillary tubes is investigated both numerically and experimentally. They were used following friction factor equations and developed model including metastable region for both liquid and two-phase regions.

For liquid region (M&N equation):

$$f_{sp} = \frac{0.192 \left(\frac{d}{D_c} \right)^{.05}}{\left[\text{Re} \left(\frac{d}{D_c} \right)^{2.5} \right]^{\frac{1}{6}}} X \left\{ 1 + \frac{0.068}{\left[\text{Re} \left(\frac{d}{D_c} \right)^{2.5} \right]^{\frac{1}{6}}} \right\} \quad (2.3)$$

For two phase region (GIRI equation)

$$f_{tp} = 1.1258 / \left[\text{Re}^{0.1938} \left(\frac{D_c}{d} \right)^{0.5391} \right] \quad (2.4)$$

For both liquid and two phase region (M&N equation):

$$f_1 = \frac{0.192 \left(\frac{d}{D_c} \right)^{.05}}{\left[\text{Re} \left(\frac{d}{D_c} \right)^{2.5} \right]^{\frac{1}{6}}} X \left\{ 1 + \frac{0.068}{\left[\text{Re} \left(\frac{d}{D_c} \right)^{2.5} \right]^{\frac{1}{6}}} \right\} \quad (2.5)$$

Both for liquid and two-phase region:

$$f_{sp,tp} = \frac{\omega \left(\frac{d}{D_c} \right)^{0.5}}{\left[\text{Re} \left(\frac{d}{D_c} \right)^{2.5} \right]^{\frac{1}{6}}} X \left\{ 1 + \frac{\psi}{\left[\text{Re} \left(\frac{d}{D_c} \right)^{2.5} \right]^{\frac{1}{6}}} \right\} \quad (2.6)$$

New developed C–M&N method for coiled friction factor gives quite good prediction of mass flow rate with the average deviation of $\pm 5\%$. Experiments on several capillary tubes with different length, inner diameter and coiled diameter were conducted to validate the model under various operating conditions. The test results showed that mass flow rate increases with increase of coiled diameter. However, beyond $D = 300$ mm (coiled diameter) the mass flow rate changes little. The mass flow rate of a capillary tube with coiled diameter of 40 mm is approximately 10% less than that of the straight capillary tube. Therefore, with coiling effect considered, the tube length should be slightly shortened to match the required system mass flow rate.

Guobing.Z and Yufeng.Z, (2006b) confirms the mass flow rate hysteresis in a coiled adiabatic capillary tube and it was more prominent than in the straight tube due to the disturbance generated from the secondary flow caused by the centrifugal force. Also, for the increasing sub cooling path, the measured data tend to become consistent even though the starting point states were different. However, for the decreasing sub cooling paths, the data points were much more dispersive due to their different initial point states. Measured temperature distributions along the tube length confirm that the significant scattering in mass flow rate data was caused by variation in the flash point location.

Further, in the capillary tube, the refrigerant flashes earlier than with decreased coiled diameter no matter whether the path is sub cooling increasing or sub cooling decreasing, thus leading to a smaller mass flow rate. With the hysteresis effect taken into account, when experimental results were compared with model predictions, data for the sub cooling increasing path should be applied due to their consistency and reproducibility in that case. In fact, for an actual vapor compression system, capillary tube inlet sub cooling increases gradually during a start-up operation.

Park *et al.* (2007) tested the performance of straight and coiled capillary tubes with R22. They were measured the performance by varying the operating conditions, tube geometries, and coiled shape. The mass flow rates of the coiled capillary tubes decreased by 5-16% more than those of the straight capillary tubes under the same operating conditions due to increased flow friction resulting from strong coiled effects. These results were confirmed by numerical simulation of the performance of the coiled capillary tubes. A generalized correlation to predict the refrigerant mass flow rate through both straight and capillary tubes was derived by implementing

dimensionless parameters that were generated using the Buckingham Ω -theorem considering the effects of tube inlet conditions, coiled tube geometries, and refrigerant properties. The coiled effects of the coiled capillary tube were considered by introducing the capillary equivalent length L_e . In addition, the average and standard deviations of the present correlation were 0.24% and 4.4%, respectively. The predictions given by their co-relation were 4.5% higher than those of ASHRAE correlation.

Khan *et al.* (Jan. 2008) presented an experimental study for the flow of R-134a inside an adiabatic spirally coiled capillary tube. The effect of various geometric parameters like capillary tube diameter, length and coil pitch for different capillary tube inlet sub cooling's on the mass flow rate of R-134a through the spiral capillary tube geometry have been investigated. The following conclusions have been carried out from their experimental study:

1. The effect of taps on the mass flow rate through the capillary tube is insignificant. Virtually, there is no effect of pressure taps on the refrigerant mass flow rate in straight and spiral capillary tube as well.
2. Parametric study has been conducted for the mass flow rate of R-134a through the capillary tubes of straight and coiled geometry. The effect coiling on refrigerant causes the refrigerant mass flow rate to reduce by 5–15%.
3. The semi-empirical correlations to predict the refrigerant mass flow rate through straight as well as spiral capillary tube have been proposed.

Khan *et al.*, (Sep. 2008) also investigated experimentally flow of R-134a through an adiabatic helically coiled capillary tube and almost same results have been given as in case of spirally coiled capillary tube. They also investigated the effect of coil pitch on the refrigerant mass flow rate and it was found that coiling has almost negligible effect on mass flow rate of capillary tube and reduces the mass flow rate by 5% to 16%.

2.2 Review of numerical work

Numerical modeling is an effective tool to predict the flow characteristics of refrigerant in the capillary tube without conducting laborious experimental work. Therefore, a number of numerical models had been developed by different investigators to study the flow of various

types of refrigerants through the capillary tubes. But unfortunately there is very limited literature on numerical investigation of coiled capillary tubes.

O.Gercia-Valladares. (2007) presented their paper on numerical simulation and experimental validation of coiled adiabatic capillary tubes. The friction factor used by them was evaluated from the expression proposed by Guobing.Z and Yufeng.Z (2006) with different coefficient considering the tube wall roughness.

$$f = \frac{C_1 \left(\frac{d}{D_c} \right)^{0.5}}{\left[\text{Re} \left(\frac{d}{D_c} \right)^{2.5} \right]^{\frac{1}{6}}} \times \left\{ 1 + \frac{C_2}{\left[\text{Re} \left(\frac{d}{D_c} \right)^{2.5} \right]^{\frac{1}{6}}} \right\} \quad (2.7)$$

Where

$$C_1 = 1.88411177 \times 10^{-1} + 8.52472168 \times 10(\varepsilon/d) - 4.63030629 \times 10^4(\varepsilon/d)^2 + 1.31570014 \times 10^7(\varepsilon/d)^3$$

$$C_2 = 6.79778633 \times 10^{-2} + 2.53880380 \times 10(\varepsilon/d) - 1.06133140 \times 10^4(\varepsilon/d)^2 + 2.54555343 \times 10^6(\varepsilon/d)^3$$

They developed a four region numerical model in which they considered liquid region, metastable single phase, metastable two-phase and equilibrium two phase region. The simulation has been implemented on the basis of a finite volume formulation of the governing equations. The solution has been carried out using an implicit step-by-step numerical scheme. The accuracy of the detailed simulation model is demonstrated in that paper was due to numerical results were compared with a wide range of experimental data from the technical literature show a good degree of agreement with the mass flow rate obtained.

Khan *et al.* (2008) has been developed a mathematical model to predict the performance of a helical capillary tube under adiabatic flow conditions. The proposed model can predict the length of the adiabatic helical capillary tube for a given mass flow rate or the mass flow rate through a given length of capillary tube. The effect of parameters like condensing pressure, degree of sub

cooling, pitch of helix and the coil diameter has been studied for the flow of refrigerant R-134a through the adiabatic helical capillary tube. A capillary tube selection chart has been developed, using the proposed model, to predict the mass flow rate of refrigerant R-134a through a capillary of size 1.07 mm diameter and 2 m length. Their model flow has been divided in three distinct regions, viz., single-phase sub cooled liquid, metastable non-equilibrium flow and two-phase liquid vapor region. In adiabatic capillary tube, the refrigerant expands from high pressure side to low pressure side adiabatically. The refrigerant usually enters the capillary tube in a sub cooled condition. As the liquid refrigerant flows through the capillary, the pressure drops linearly due to friction. As the pressure falls below the saturation pressure corresponding to refrigerant temperature, ideally a part of refrigerant should have been flashed into vapors. But in actual scenario the flow stays in thermodynamic non-equilibrium liquid state, called metastable flow, below its saturation pressure under superheated condition. As a result of it, the vaporization is delayed and flashing point shifts further downstream. The possible reasons of the metastability may be that finite amount of superheat is required for the formation of first bubble. The direct consequence of metastability is the increase in critical mass flow rate which delays the flash point and the choking point. In their mathematical model they convert helical capillary into

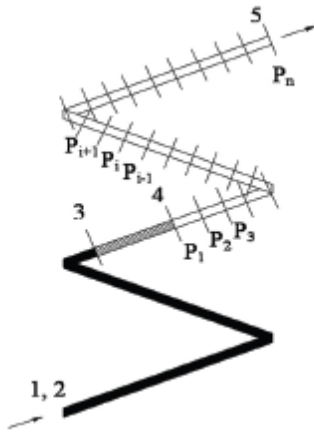


Figure 2.3 Computational domain capillary tube

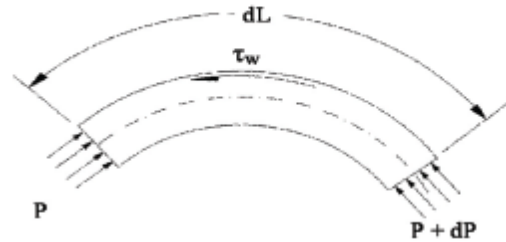


Figure 2.4 Force acting on a fluid element

a computational elements and apply basic governing equations to these elements as shown in figure 2.3 and 2.4. And Dukler's viscosity co-relation were used to predict the fluid flow.

Khan *et al.* (Sep. 2007) again analyze the flow characteristic of refrigerant flowing inside an adiabatic spiral capillary tube. The model predicts the length of two types of tubes, straight and spiral adiabatic capillary tubes. Their proposed model was based on the homogenous two-phase flow model, which predicts the length of the adiabatic capillary tubes as a function of refrigerant mass flow rate, capillary tube diameter, degree of sub cooling at capillary inlet, internal surface roughness, and the pitch of the Archimedean spiral. The existence of sub cooled liquid at the entry of the capillary tube requires the computation of single-phase and then two-phase lengths of the tube. The McAdams viscosity correlation has been used to evaluate the two-phase viscosity of the expanding refrigerant in the latter part of the capillary tube. All the thermo physical and transport properties of the refrigerants are evaluated by the REFPROP (NIST. REFPROP 7.0), which is based on the Carnahan-Starling-DeSantis equation of state. The simulation results were validated with the experimental findings of previous researchers. The performance of two geometries of adiabatic capillary tube was compared, and it is established that for the same state of refrigerants at the inlet and exit of the adiabatic capillary, spiral capillary is found to have a shorter length. Parametric study of the adiabatic capillary tubes is also carried out.

S.Wongwises *et al.* (2010) presented the effects of various geometries of helical capillary tubes on the flow characteristics of alternative refrigerants flowing through adiabatic helical capillary tubes. The theoretical model is based on the conservation of mass, energy and momentum of fluids in the capillary tube. The two-phase flow model developed was based on a homogenous flow assumption. The model was validated by comparing it with the experimental data of published in literature for R-22, particularly various pairs of refrigerants. It was found conventional refrigerants had lower capillary lengths than alternative refrigerants. For all pairs, the numerical results showed that the traditional refrigerants consistently gave lower pressure drops for both single-phase and two-phase flows, which resulted in longer tube lengths. The results show that coil diameter variation (less than 300 mm) for helical capillary tube geometries affected the length of helical capillary tubes. However, pitch variation (more than 300 mm) had no significant effect on the length of helical capillary tubes. This adiabatic helical capillary tube model can be used to integrate system models working with alternative refrigerants for design and optimization.

S.Wongwises *et al.* (2011) presented a numerical study of the flow characteristics of refrigerants flowing through adiabatic helically coiled capillary tubes. The two-phase flow model developed was based on the homogeneous flow assumption. The viscosity model was also based on recommendations from the literature. This paper presents a numerical investigation of the flow characteristics of helical capillary tubes compared with straight capillary tubes. The homogeneous two-phase flow model developed was based on the conservation of mass, energy, and momentum of the fluids in the capillary tube. This model is validated by comparing it with the experimental data of both straight and helical capillary tubes. Comparisons of the predicted results between the straight and helical capillary tubes are presented, together with the experimental results for straight capillary tubes obtained by previous researchers. The results show that the refrigerant flowing through the straight capillary tube provides a slightly lower pressure drop than that in the helical capillary tube, which resulted in a total tube length that was longer by about 20%. In addition, for the same tube length, the mass flow rate in the helical capillary tube with a coil diameter of 40 mm is 9% less than that in the straight tube.

2.3 Types of mathematical models

2.3.1 Homogeneous flow model The majority of the numerical models available in the literature have considered the two-phase flow as homogeneous flow. In homogeneous two-phase flow, it is assumed that there is no slip between the two phases, i.e., the two phases liquid and vapor move with the same velocity.

2.3.2 Separate flow model In separated flow model, it is assumed that there exists slip between the two phases and, when the conservation equations are applied for the two-phase mixture, a variable called void fraction is introduced. Unlike homogeneous flow model, which requires experimental information of the friction effect, the separated flow model requires information of the void fraction as well, in addition to friction effects.

2.3.3 Drift flux models In the drift flux model, the conservation equation is formulated by considering the two phase region as a mixture of two phases. Therefore, the formulation for two phase flow is expressed in terms of four field equations: three for the mixture (continuity, momentum and energy) and one for the drift velocity for one of the phases.

2.4 Conclusion from literature review

- The flow of various refrigerants through adiabatic straight capillary tubes has been studied extensively by a number of researchers. The studies include both experimental and numerical investigations.
- A number of empirical correlations to predict the refrigerant mass flow through a capillary are also available in the literature.
- It has been observed that a very few studies have been carried out on refrigerant flow analysis through coiled and spiral adiabatic capillary tube.
- With phasing out of conventional refrigerant due to ozone layer depletion a lot of study needed on refrigerant behavior in spiral and helical capillary tubes. This is due to fact that helical and spiral capillary tubes have been used extensively on practical grounds rather than straight one.

Chapter - III

MATHEMATICAL MODEL

A mathematical model has been developed to predict the flow of refrigerant inside a helical capillary tube. Length of helical adiabatic capillary tube can be calculated by giving the mass flow rate of particular refrigerant or vice-versa. A computer program coded in MATLAB has been developed to compute either length or mass flow rate by fixing some of parameter. The model also includes the effect of various design parameters, like capillary tube diameter, capillary tube coil diameter, degree of sub-cooling, evaporator pressure, inlet pressure, mass flow rate. The model is based on the fundamental equations of conservation of mass, energy and momentum and that the refrigerant properties (both thermodynamic and transport) are derived from the REFPROP. The mathematical model has been validating with the experimental data available in the open literature.

3.1 FORMULATION OF MATHEMATICAL MODEL

The flow of refrigerant can be divided into two distinct regions. The single phase sub cooled region and two phase region. The mathematical model is developed by using the law of conservations of mass, energy and momentum. Moreover, the model includes the effect of the condenser and evaporator temperatures, inner diameter, and degree of sub cooling and mass flow rate of refrigerant.

As shown in fig 3.1, the entry diagram of refrigerant commence at point 1 from the condenser. In the capillary tube there is some pressure drop due to entry of the refrigerant from the condenser to the capillary tube. The portion between points 2 and 3 is the single-phase sub cooled liquid region and the portion between points 3 and 4 is the two-phase region where liquid and vapor coexist. From 2 to 3 refrigerant remains in single liquid phase and vapors starts to form as it enters in two phase region. In single region pressure drop is linear and due to friction that experience by the fluid while passing through the tube. And in the two-phase region of the capillary tube, the temperature and pressure of refrigerant starts falling rapidly till the evaporator pressure or the choking point is attained.

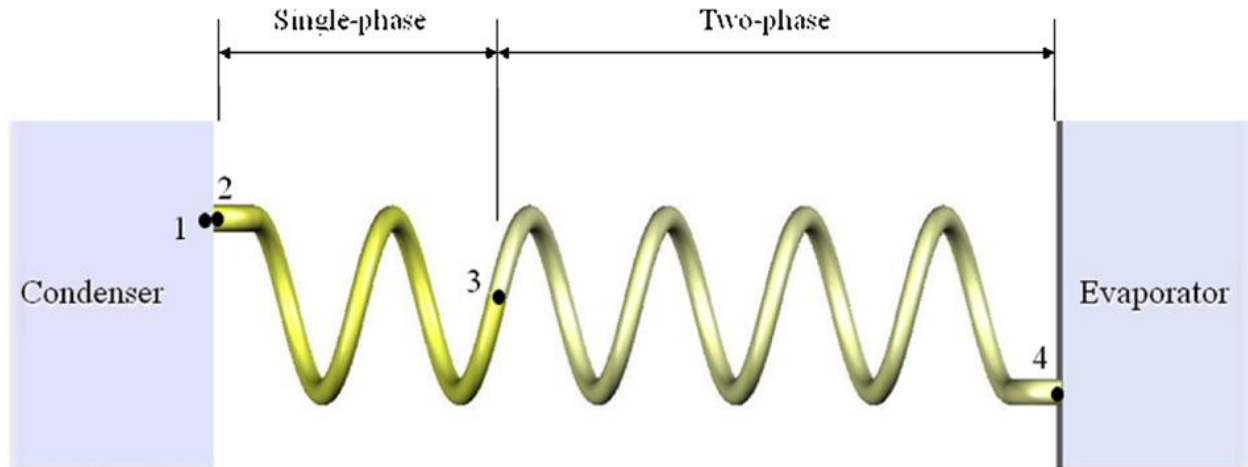


Figure 3.1 Systematic diagram of adiabatic helical capillary tube

Thus refrigerant flow has been divided into three distinct regions as follows:

1 – 2 represents pressure drop at entrance due to sudden contraction of area.

2 – 3 represents single-phase sub cooled flow region.

3 – 4 represents liquid-vapor two-phase flow region.

In order to formulate a mathematical model some assumption are taken into account which are as follows:

- The horizontal helical coiled tube has constant diameter.
- Oil free refrigerant.
- The inner diameter and surface roughness of the capillary tube are constant.
- Adiabatic and homogeneous two-phase flow.
- Non-metastable liquid region.
- One-dimensional steady flow.
- Thermodynamic equilibrium through the capillary tube.

Consider an infinitesimal fluid element of length ' dL ' within the capillary tube, shown in Fig.3.2 and applying the equations of conservation of mass, momentum and energy.

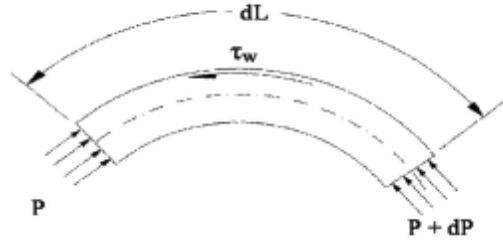


Figure 3.2 Free body diagram of fluid element of adiabatic helical capillary tube

Mass Balance

Continuity equation results into the following equation

$$m = \rho VA \text{ or } G = \frac{m}{A} = \rho V \quad (3.1)$$

Momentum Balance

On applying the principle of momentum conservation and second law gives

$$P.A - (P + dP).A - \tau_w (\pi d) dL = mdV \quad (3.2)$$

on simplification, the Equation (4.2) reduces to the following Equation (3.3)

$$dL = -\frac{2d}{f} \left(\frac{\rho dP}{G^2} + \frac{dV}{V} \right) \quad (3.3)$$

Taking log of both sides of Equation (3.1) and then differentiating and simplifying

$$-\frac{dV}{V} = \frac{d\rho}{\rho} \quad (3.4)$$

Equation (3.3) reduces to

$$dL = \frac{2d}{f} \left(\frac{\rho dP}{G^2} - \frac{d\rho}{\rho} \right) \quad (3.5)$$

Energy Balance

On applying the steady flow energy equation for adiabatic flow with no external work and neglecting the elevation difference we have

$$\delta q - \delta w = dh + VdV + gdz \quad (3.6)$$

3.1.1 Single phase region

In order to calculate the single phase length, the pressure drop at inlet due to sudden contraction is considered. Liquid is incompressible (density constant) and capillary tube area is constant.

By integrating equation (3.5) length of single phase region is given by

The Pressure drop at the entrance is given by

$$P_1 - P_2 = k \frac{\rho V^2}{2} \quad (3.7)$$

Where k is the entrance loss coefficient (for square edged, k=0.5).The steady flow equation between point 2 and 3 can be expressed as:

$$\frac{P_2}{\rho_2 g} + \frac{V_2^2}{2g} + Z_2 = \frac{P_3}{\rho_3 g} + \frac{V_3^2}{2g} + Z_3 + f_{sp} \frac{L_{sp}}{d_i} \frac{V^2}{2g} \quad (3.8)$$

As we know fluid is incompressible so

$$m = \rho VA = \rho_2 AV_2 = \rho_3 AV_3 \quad (3.9)$$

By rearranging equation (3.8) and (3.9) we have

$$P_2 = P_3 + \rho g (Z_3 - Z_2) + \left(\frac{f_{sp} L_{sp}}{d_i} \right) \left(\frac{\rho V^2}{2} \right) \quad (3.10)$$

For same elevation we have $Z_2=Z_3$, Substituting equation (3.10) into (3.7) which gives:

$$L_{sp} = \frac{d_i}{f_{sp}} \left[\frac{2\rho}{G^2} (P_1 - P_2) - k - 1 \right] \quad (3.11)$$

Where $G = \frac{m}{A} = \rho V$

Friction factor is an important parameter and available friction factors correlations are in large numbers and some of them taken in the account for developing the mathematical model for different refrigerants. In the presented work model three of friction factor correlations have been used for development of the mathematical model taken from Guobing.Z and Yufeng.Z (2006).

For liquid region (M&N equation):

$$f_{sp} = \frac{0.192 \left(\frac{d}{D_C} \right)^{.05}}{\left[\text{Re} \left(\frac{d}{D_C} \right)^{2.5} \right]^{\frac{1}{6}}} X \left\{ 1 + \frac{0.068}{\left[\text{Re} \left(\frac{d}{D_C} \right)^{2.5} \right]^{\frac{1}{6}}} \right\} \quad (3.12)$$

For two phase region (GIRI equation)

$$f_{tp} = 1.1258 / \left[\text{Re}^{0.1938} \left(\frac{D_C}{d} \right)^{0.5391} \right] \quad (3.13)$$

For both liquid and two phase region (M&N equation):

$$f_{sp,tp} = \frac{0.192 \left(\frac{d}{D_C} \right)^{.05}}{\left[\text{Re} \left(\frac{d}{D_C} \right)^{2.5} \right]^{\frac{1}{6}}} X \left\{ 1 + \frac{0.068}{\left[\text{Re} \left(\frac{d}{D_C} \right)^{2.5} \right]^{\frac{1}{6}}} \right\} \quad (3.14)$$

Both for liquid and two-phase region:

$$f_{sp,tp} = \frac{\omega \left(\frac{d}{D_C} \right)^{0.5}}{\left[\text{Re} \left(\frac{d}{D_C} \right)^{2.5} \right]^{\frac{1}{6}}} X \left\{ 1 + \frac{\psi}{\left[\text{Re} \left(\frac{d}{D_C} \right)^{2.5} \right]^{\frac{1}{6}}} \right\} \quad (3.15)$$

Different values for study can be taken from the table 3.1 Guobing.Z and Yufeng.Z (2006).

Coil diameter(d) mm	ξ/d	ω	Ψ
1.0	0.00025	0.207	0.0737
1.2	0.0004	0.216	0.0766
1.4	0.00122	0.248	0.0878
1.6	0.0014	0.253	0.0897
2.2	0.00116	0.245	0.0885

3.1.2 Two phase flow region

In this region vapor and liquid fluid flows through helical adiabatic capillary tube. Refrigerant fluid flow is homogeneous means vapor and liquid move with same velocity. In two phase region capillary tube has been divided into number of elements. The following equations are based on the control volume consideration in two phase region.

By conservation of mass we have

$$m = \frac{AV_i}{v_i} = \frac{AV_{i+1}}{v_{i+1}} \quad (3.16)$$

Where v_i is the specific volume of fluid at any point.

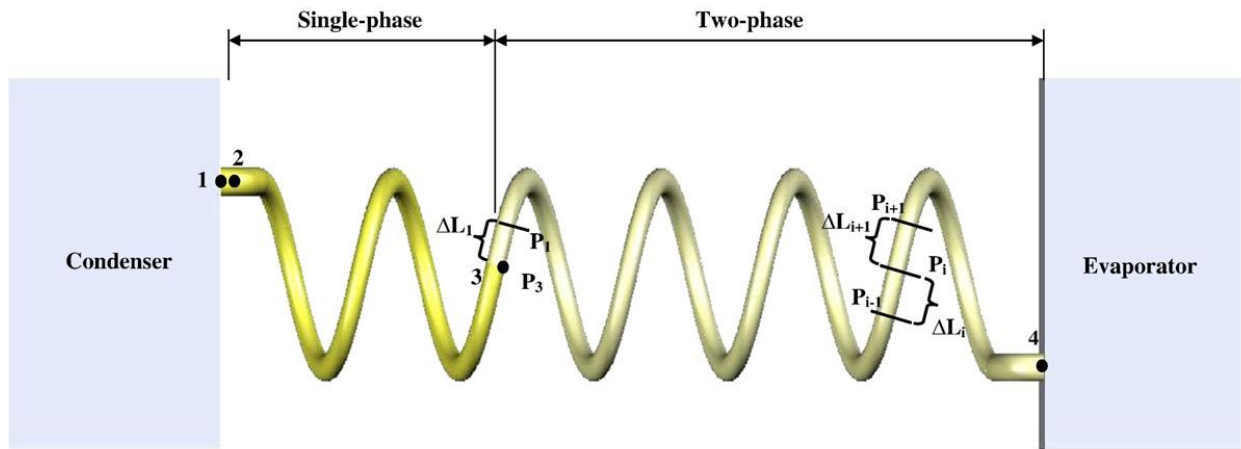


Figure 3.3 Systematic fluid element considerations in two phase flow in adiabatic helical capillary tube

By neglecting the elevation difference, the conservation of energy for steady state adiabatic condition without external work can be expressed as follows:

$$\left(h_3 + \frac{V_3^2}{2} + gZ_3 \right) = \left(h_i + \frac{V_i^2}{2} + gZ_i \right) \quad (3.17)$$

$$h + \frac{V^2}{2} = \text{Constant} \quad (3.18)$$

Where h and V are the enthalpy and velocity of fluid at any point, respectively.

Due to fact that as the refrigerant flows through the capillary tube, the pressure gradually drops and the liquid flashes into vapors arising from the reduced pressure. Hence,

$$h_i = h_{fi} \left(- x_i \right) h_{gi} x_i \quad (3.19)$$

$$v_i = v_{fi} \left(- x_i \right) v_{gi} x_i \quad (3.20)$$

Also, $m = \rho AV = \text{constant}$

$$V = \frac{m}{\rho A} = \frac{G}{\rho} = Gv \quad (3.21)$$

The energy balance between point 3 and 4 can be calculated by putting the equation 3.19, 3.20 and 3.21 into equation 3.18 and is given by

$$h_3 + \frac{V_3^2}{2} = h_f + x \left(h_g - h_f \right) + \frac{G^2}{2} \left(v_f \left(- x \right) v_g x \right) \quad (3.22)$$

By rearranging we have

$$\left[\left(v_g - v_f \right) \frac{G^2}{2} \right] x^2 + G^2 v_f (v_g - v_f) x + \left[\frac{G^2 v_f^2}{2} - h_3 - \frac{V_3^2}{2} + h_f \right] = 0 \quad (3.23)$$

And the dryness fraction can be expressed in the quadratic equation as

$$x = \frac{-h_{fg} - G^2 v_f v_{fg} + \sqrt{\left(G^2 v_f v_{fg} + h_{fg} \right)^2 - 2G^2 v_{fg}^2 \left(\frac{G^2 v_f^2}{2} - h_3 - \frac{V_3^2}{2} + h_f \right)}}{G^2 v_{fg}^2} \quad (3.24)$$

Where $h_{fg} = h_g - h_f$ and $v_{fg} = v_g - v_f$

Again conservation of momentum can be expressed by using the element of fluid shown in fig 3.2.

$$\left(P \frac{\pi d_i^2}{4} \right) - \left(P + dP \right) \frac{\pi d_i^2}{4} - \tau_w \pi d_i dL = mdV \quad (3.25)$$

Where τ_w is the wall shear stress and is given by:

$$\tau_w = \frac{f_{tp} \rho V^2}{8} \quad (3.26)$$

And the two phase friction factor can be calculated from the three method already discussed.

Now by putting equation 3.26 in Equation 3.25 we have

$$-\frac{\pi d_i^2}{4} dp - \frac{f_{tp}}{8} \rho V^2 d_i \pi dL = mdV \quad (3.27)$$

And in modified form we have

$$dL = -\frac{d_i}{f_{tp}} \left[\frac{2dp}{\rho V^2} + \frac{2mdV}{\rho A V^2} \right] \quad (3.28)$$

For constant mass flow rate

$$\frac{dV}{V} = -\frac{d\rho}{\rho} \quad (3.29)$$

Substituting Equation 3.29 into 3.28 we have

$$dL = \frac{2d_i}{f_{tp}} \left[\frac{-\rho dp}{\rho V^2} + \frac{d\rho}{\rho} \right] \quad (3.30)$$

Fig 3.2 shows the systematic division of adiabatic helical capillary tube between point 3 and 4.

P_3 is known and pressure at any section i can be calculated as follows:

$$P_i = P_3 - i\Delta P \quad (3.31)$$

Now we can calculate pressure (P_i) and the quality (x_i) from equation 3.24. So entropy at each section is given by

$$s_f = s_{fi} \left(1 - x \right) + s_{gi} x \quad (3.32)$$

In two phase region Reynolds number is given by

$$Re_{tp} = \frac{Vd}{\mu_{tp} v_{tp}} \quad (3.33)$$

Where μ_{tp} is the two phase viscosity which can be calculated by two phase viscosity models as given in table 3.1. But in present study we will take duklers viscosity model.

Table 3.2 Two-phase viscosity correlation models

<i>Researchers name</i>	<i>viscosity models</i>
<i>McAdams (1942)</i>	$\frac{1}{\mu_{tp}} = \frac{x}{\mu_g} + \frac{1-x}{\mu_f}$
<i>Cicchitti (1960)</i>	$\mu_{tp} = x\mu_g + (1-x)\mu_f$
<i>Dukler et al. (1964)</i>	$\mu_{tp} = \frac{xV_g\mu_g + (1-x)v_f\mu_f}{xv_g + (1-x)v_f}$
<i>Beattie et al. (1981)</i>	$\mu_{tp} = \alpha_{tp}\mu_g + (1-\alpha_{tp})(1+2.5\alpha_{tp})\mu_f \text{ where}$ $\alpha_{tp} = \frac{xV_g}{v_f + xv_{fg}}$
<i>Lin et al. (1991)</i>	$\mu_{tp} = \frac{\mu_g\mu_f}{x\mu_g + x^{1.4}(\mu_f - \mu_g)}$

In present mathematical model, Two phase viscosity model of *Dukler's (1964)* has been used. And velocity (V) is given by

$$V = Gv_{tp} = G \left[xv_g + (1-x)v_f \right] \quad (3.34)$$

As the flow progress the gradual increase in entropy is obtained along the adiabatic helical capillary tube. When the maximum value of entropy in the helical capillary tube reaches the sonic velocity is equal to the refrigerant fluid velocity and flow gets chocked. And program will end the calculation at this point of maximum entropy. And pressure of the element $(P_i)_{s \max}$ compared to the pressure of evaporator $(P_{\text{evap.}})$ when entropy has a maximum value attained.

if $(P_i)_{s \max} = P_{\text{evap.}}$ then $P_4 = P_{\text{evap.}}$

if $(P_i)_{s \max} \neq P_{\text{evap.}}$ then $P_4 = (P_i)_{s \max}$

Two phase length can be calculated by integrating the equation 3.30 we have

$$L_{tp} = 2d \left(\frac{-1}{G^2} \int_{P_3}^{P_{s,max}} \frac{\rho}{f_{tp}} dP + \int_{P_3}^{P_{s,max}} \frac{d\rho}{\rho f_{tp}} \right) \quad (3.35)$$

And capillary length of each section is given by

$$\Delta L_i = \frac{2d_i}{f_{tp,i}} \left(\frac{-\rho_i \Delta P}{G^2} + \frac{\Delta \rho}{\rho_i} \right) \quad (3.36)$$

Where, ρ_i and $F_{tp,i}$ are mean density and mean friction factor respectively over the 'ith' element in two phase region. And final length will be sum of single phase and two phase length.

$$L = L_{sp} + L_{tp} \quad (3.37)$$

Chapter - IV

RESULT AND DISCUSSION

4.1 VALIDATION OF MATHEMATICAL MODEL

In the proposed model, the results obtained from the developed numerical models are compared with experimental results of previous researcher's. The simulated results has been validating for adiabatic helical capillary tube measured by Mittal *et al.* (2009), Kim *et al.* (2002) and Khan *et al.* (2008). Predicted mass flow rate has been compared with the experimental mass flow rate under different conditions.

Table 4.1: Details for experimental data of adiabatic helical capillary tube to validate the model

Parameters	Mittal <i>et al.</i> (2009)	Kim <i>et al.</i> (2002)	Khan <i>et al.</i> (2008)
Refrigerant	R-407 C	R-407C,R-410A	R-134 a
Capillary tube length (L), m	1.00,2.00	1.00	2.00,3.00
Capillary tube diameter (d), mm	1.02,1.27	1.5	1.4
Condenser Pressure (P_{cd}), °C	16.4,18.6,14.7	19.7,27.2	7.23
Degree of subcooling (ΔT_{sub}), °C	3-12	3-12	3-18
Coil diameter (Dc)	60,100,140	40,120,200	140

4.1.1 Validation of mathematical model with Mittal *et al.* (2009) experimental data for R-407 C with coil diameter 60 mm.

Fig.4.1 shows comparison of experimental data of Mittal *et al.* (2009) with those predicted by present models for condenser pressure of 16.4 bar. It has been drawn with capillary inlet sub cooling of refrigerant as abscissa and refrigerant mass flow as ordinate. As inlet sub cooling is increased from 2 °C to 12 °C, the refrigerant mass flow rate is increased nearly by 25 percent. This is due to the fact that an increase in inlet sub cooling will increase the length of liquid region in the capillary tube. It is a known fact that the resistance offered to the fluid flow is low in the liquid region of capillary as compared to that in the two-phase liquid-vapor flow region. Therefore, increase in refrigerant mass flow rate can be associated with increase in liquid length of the capillary tube. Helical capillary tube Length, coil diameter, Evaporator pressure and tube

diameter are 2 m, 60 mm, 6.22 bar and 1.02 mm respectively. It has been observed that the mass flow rate increases with increase in degree of sub cooling. Prediction made by C-M&N equation is the closest in given set of condition with an average error of 0.37 %. As shown in the figure M&N equation also gives the close prediction to the experimental results. Prediction made by M&N+GIRI overestimated the mass flow rate of the refrigerant.

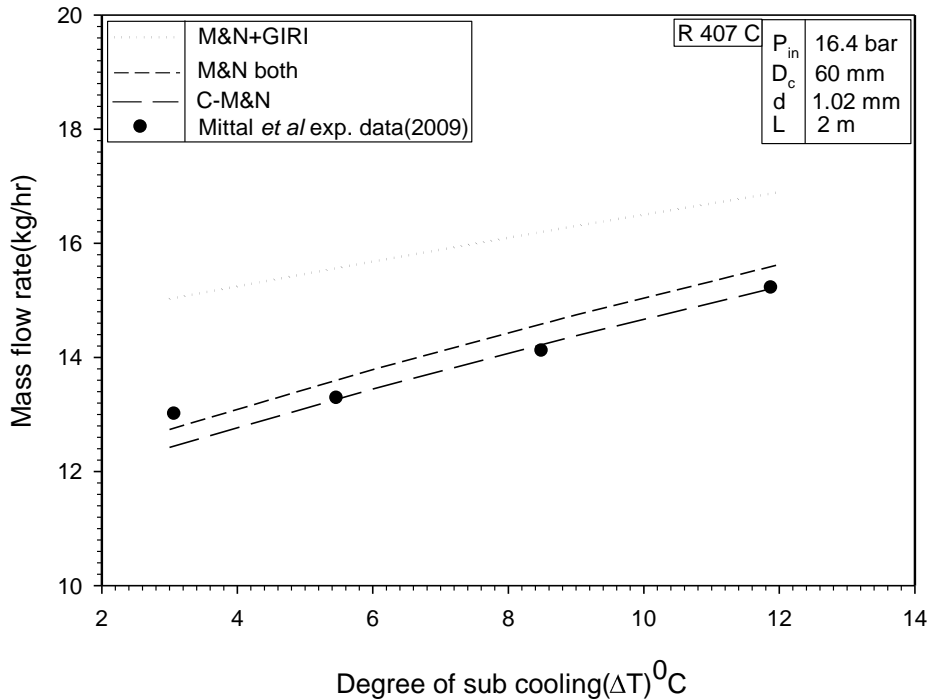


Fig.4.1: Comparison of Mittal *et al.* (2009) experimental data with present numerical results at condenser pressure of 16.4 bar for the flow of R-407 C with coil diameter 60 mm.

4.1.2 Validation of mathematical model with Mittal *et al.* (2009) experimental data for R-407 C with coil diameter 100 mm.

Fig.4.2 shows comparison of Mittal *et al.* (2009) experimental data with present models for condenser pressure of 16.4 bar. It has been drawn with capillary inlet sub cooling of refrigerant as abscissa and refrigerant mass flow as ordinate. It has been noted that mass flow rate increases with increase in inlet sub cooling. The closest estimate here is given by the M&N equation for both single and two phase flow which gives an average error of -2.04 % for condenser pressure of 16.4 bar. Prediction made by M&N+GIRI overestimated the mass flow rate of the refrigerant. Helical capillary tube Length, coil diameter, Evaporator pressure and tube diameter are 2 m, 100, 6.22 bar mm and 1.02 mm respectively.

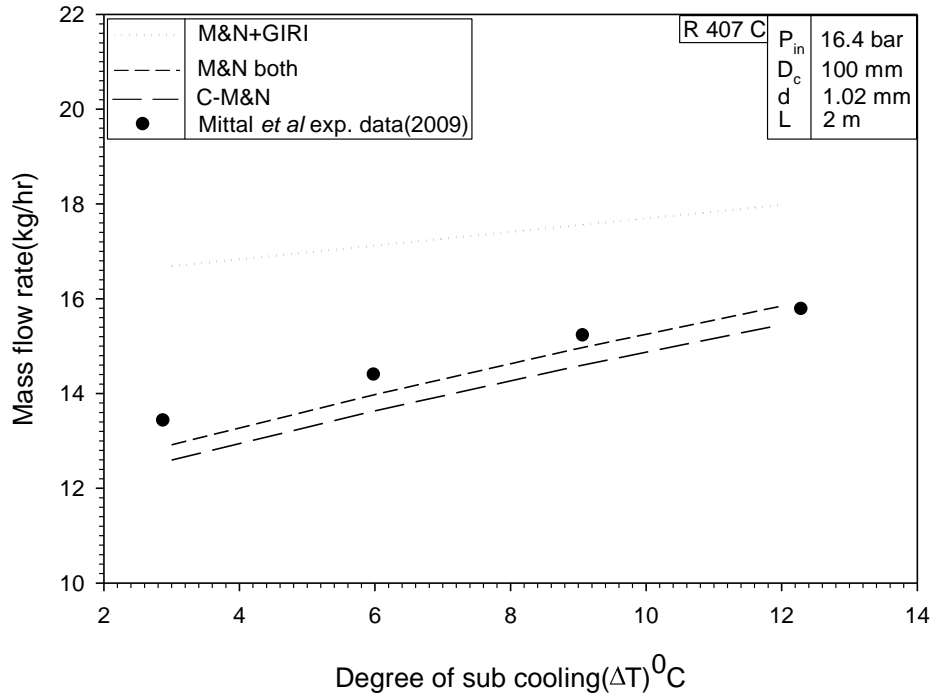


Fig.4.2: Comparison of Mittal *et al.* (2009) experimental data with present numerical results at condenser pressure of 16.4 bar for the flow of R-407 C with coil diameter 100 mm.

4.1.3 Validation of mathematical model with Mittal *et al.* (2009) experimental data for R-407 C with coil diameter 140 mm.

Fig.4.3 shows comparison of Mittal *et al.* (2009) experimental data with present models for condenser pressure of 16.4 bar. It has been drawn with capillary inlet sub cooling of refrigerant as abscissa and refrigerant mass flow as ordinate. And again closest prediction is given by M&N equation for both single and two phase flow. Which gives an average error of -5.21 % for condenser pressure of 16.4 bar. Prediction made by M&N+GIRI overestimated the mass flow rate of the refrigerant. Helical capillary tube Length, coil diameter, Evaporator pressure and tube diameter are 2 m, 140 mm, 6.22 bar and 1.02 mm respectively.

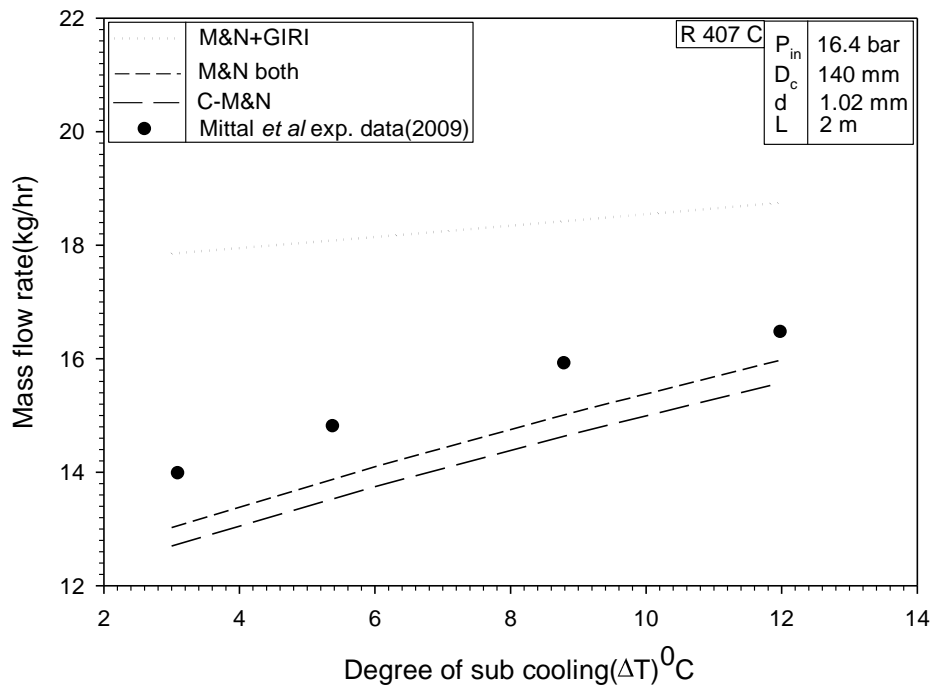


Fig.4.3: Comparison of Mittal *et al.* (2009) experimental data with present numerical results at condenser pressure of 16.4 bar for the flow of R-407 C with coil diameter 140 mm.

4.1.4 Validation of mathematical model with Mittal *et al.* (2009) experimental data for R-407 C with tube diameter 1.27 and coil diameter 60,100 and 140 mm.

Fig.4.4, 4.5 and 4.6 shows comparison of Mittal *et al.* (2009) experimental data with present models for condenser pressure of 16.4 bar. All three figures have been drawn shows that M&N equation gives the close predictions to that of the experimental results by Mittal *et al.* (2009). Mass flow rate increases with increasing degree of sub cooling. It has been noted that every time M&N + GIRI over predicted mass flow rate compared to the experimental results. Helical capillary tube Length, coil diameter, Evaporator pressure and tube diameter are 2 m, 60,100,140 mm, 4.22 bar and 1.27 mm respectively. Closest prediction is given by M&N equation for both single and two phase flow. Which gives an average error of -0.64 %, -2.24 %, -4.9 % for condenser pressure of 18.6 bar.

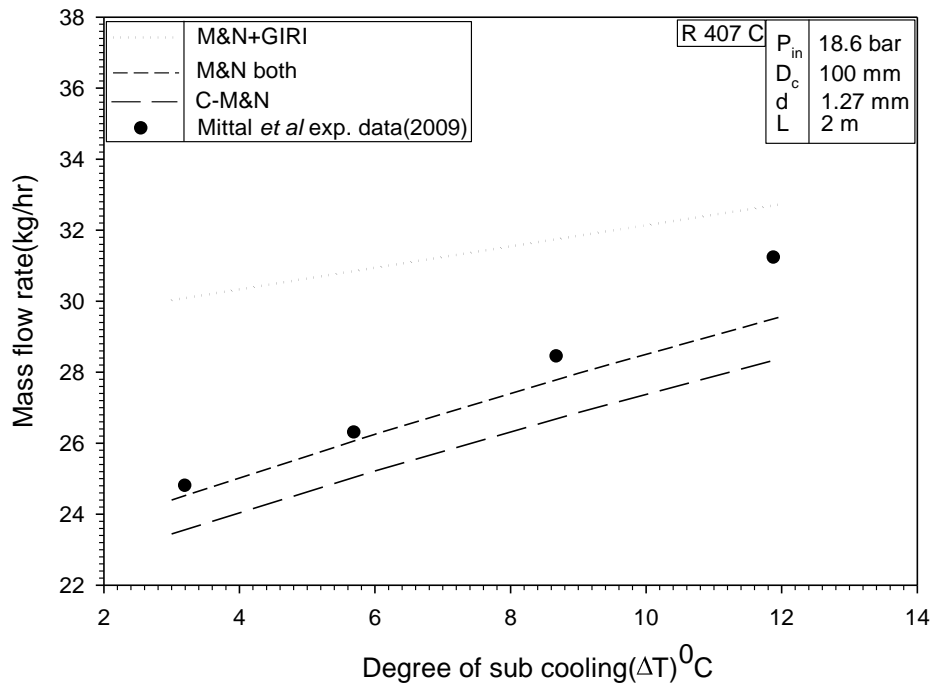
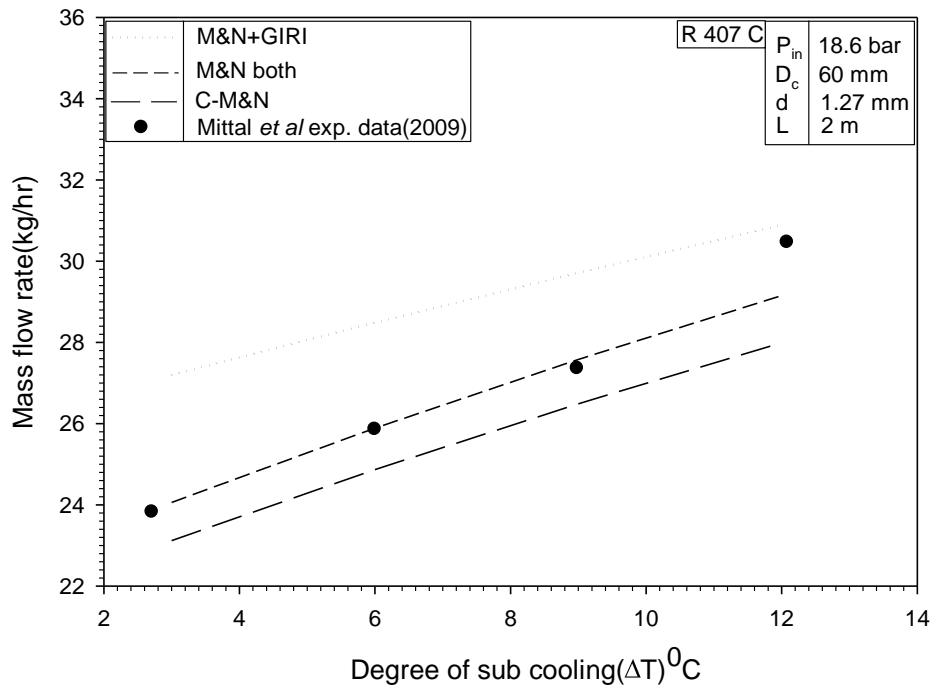


Fig.4.4 and 4.5: Comparison of Mittal et al. (2009) experimental data with present numerical at condenser pressure of 18.6 bar for the flow of R-407 C with coil diameter 60 mm and 100 mm.

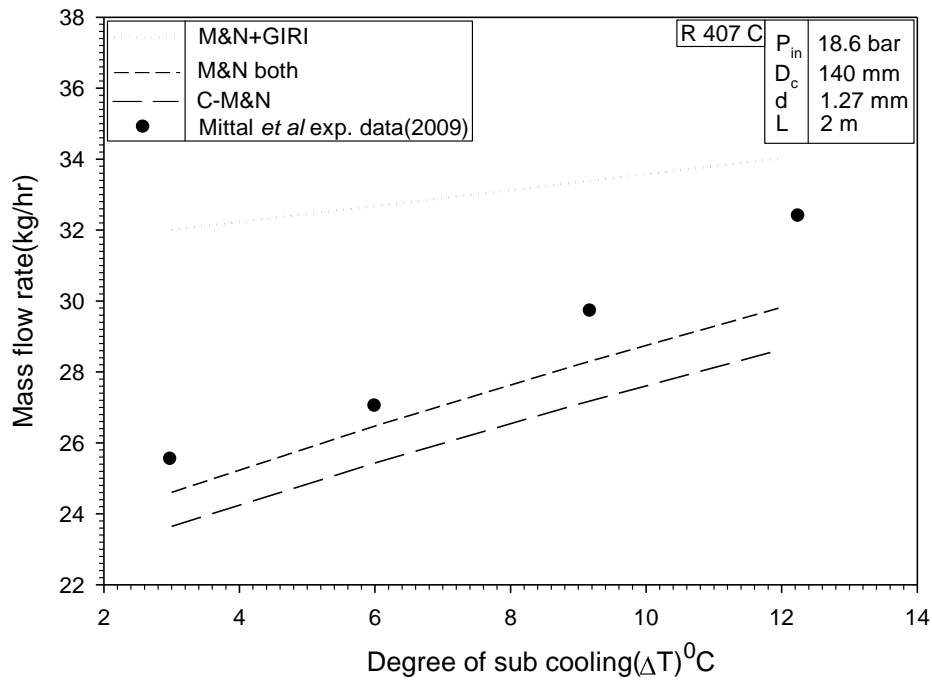


Fig.4.6: Comparison of Mittal *et al.* (2009) experimental data with present numerical results at condenser pressure of 18.6 bar for the flow of R-407 C with coil diameter 140 mm.

4.1.5 Validation of mathematical model with Mittal *et al.* (2009) experimental data for R-407 C with tube diameter 1.27 and coil diameter 60,100 and 140 mm.

Fig.4.7, 4.8 and 4.9 shows comparison of Mittal *et al.* (2009) experimental data with present models for condenser pressure of 14.7 bar. All three figures have been drawn shows that M&N equation gives the close predictions to that of the experimental results by Mittal *et al.* (2008). Mass flow rate increases with increasing degree of sub cooling. Again it has been noted that M&N + GIRI over predicted mass flow rate compared to the experimental results. Helical capillary tube Length, coil diameter, Evaporator pressure and tube diameter are 2 m, 60,100,140 mm, 4.22 bar and 1.27 mm respectively. Closest prediction is given by M&N equation for both single and two phase flow. Which gives an average error of 4.5 %, 0.709 %, -1.88 % for condenser pressure of 14.7 bar.

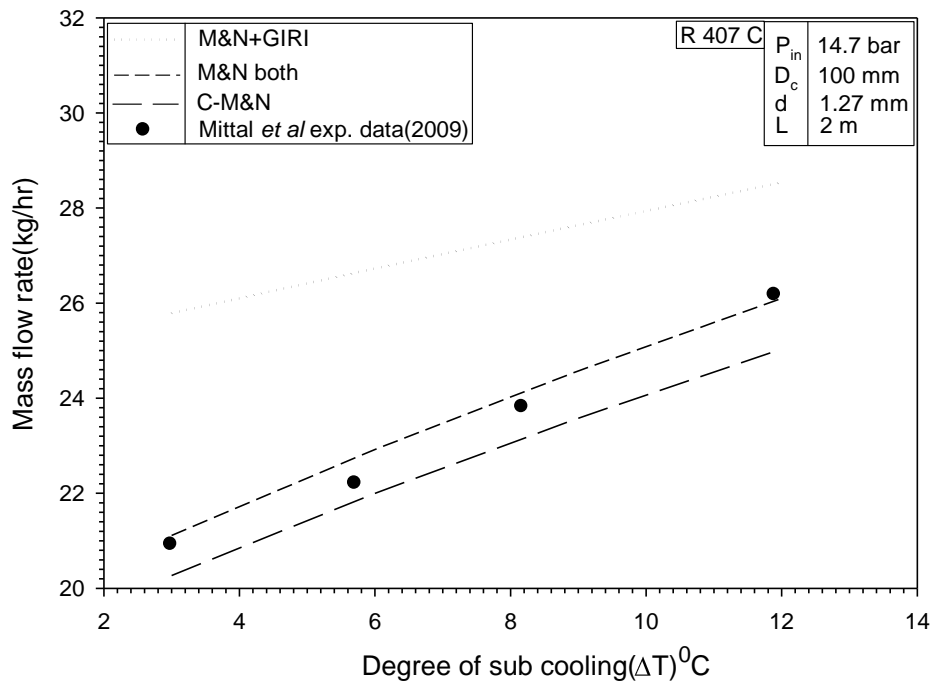
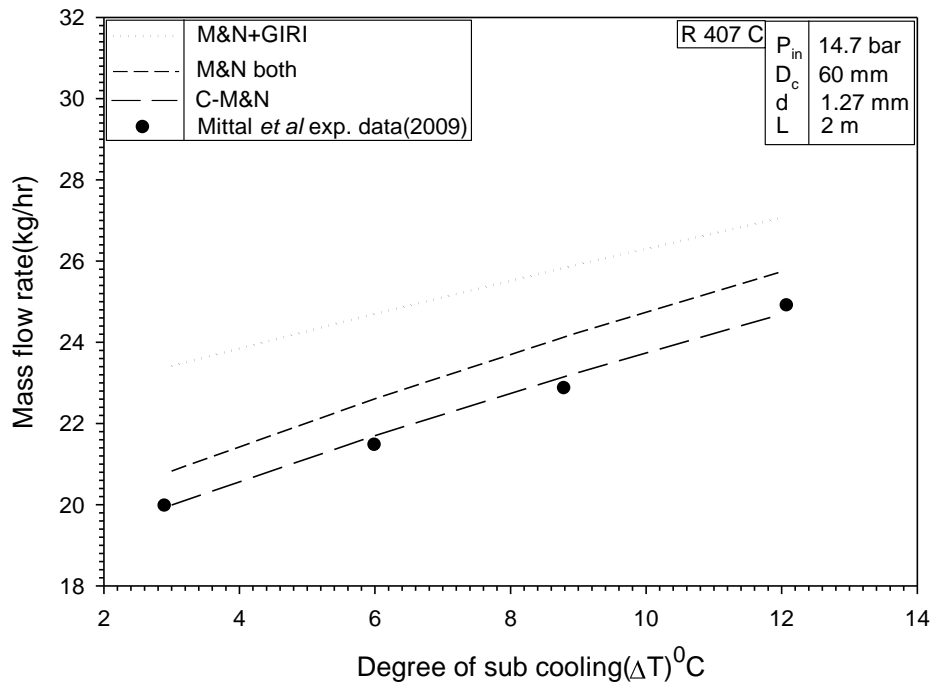


Fig.4.7 and 4.8: Comparison of Mittal et al. (2009) experimental data with present numerical results at condenser pressure of 14.7 bar for the flow of R-407 C with coil diameter 60 mm and 100 mm.

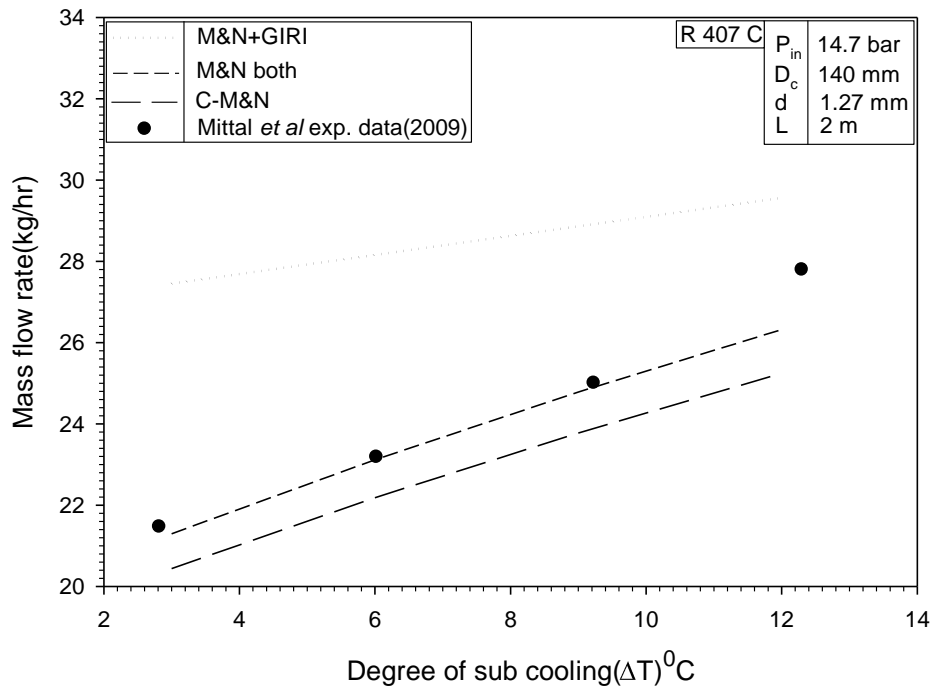


Fig.4.9: Comparison of Mittal *et al.* (2009) experimental data with present numerical results at condenser pressure of 14.7 bar for the flow of R-407 C with coil diameter 140 mm.

4.1.6 Validation of mathematical model with Kim *et al.* (2002) experimental data for R-407 C with coil diameter 40,120 and 200 mm.

Fig.4.10, 4.11 and 4.12 shows comparison of Kim *et al.* (2002) experimental data with present models for condenser pressure of 19.72 bar. In Fig. 5.10 M&N+GIRI gives the closet results and other two equations under estimate the mass flow rate of refrigerant. Figure 4.11 and 4.12 shows that M&N equation gives the close predictions to that of the experimental results by Kim *et al* (2002). Mass flow rate increases with increasing degree of sub cooling. It has been noted that M&N + GIRI over predicted mass flow rate compared to the experimental results. Helical capillary tube Length, coil diameter, Evaporator pressure and tube diameter are 1 m, 40,120 and 200 mm, 5.22 bar and 1.5 mm respectively.

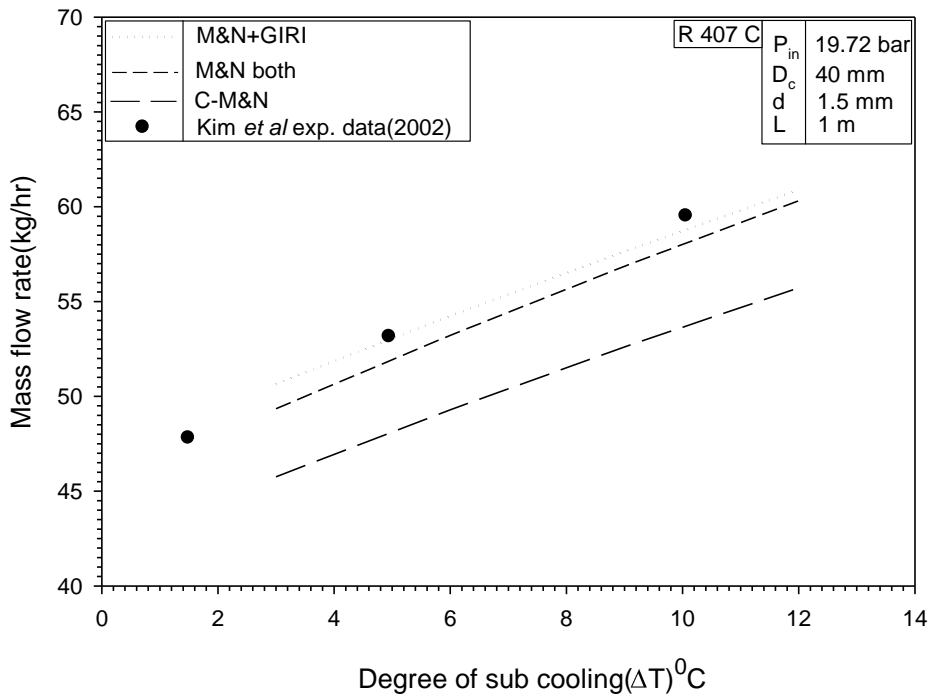
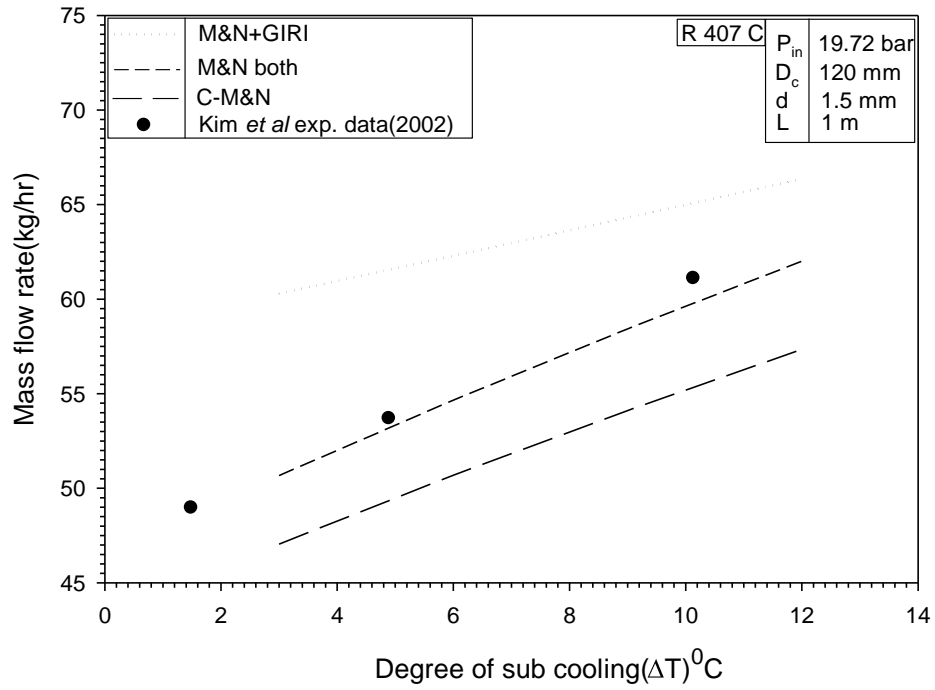


Fig.4.10 and 4.11: Comparison of Kim et al. (2002) experimental data with present numerical results at condenser pressure of 19.72 bar for the flow of R-407 C with coil diameter 40 mm and 120 mm.

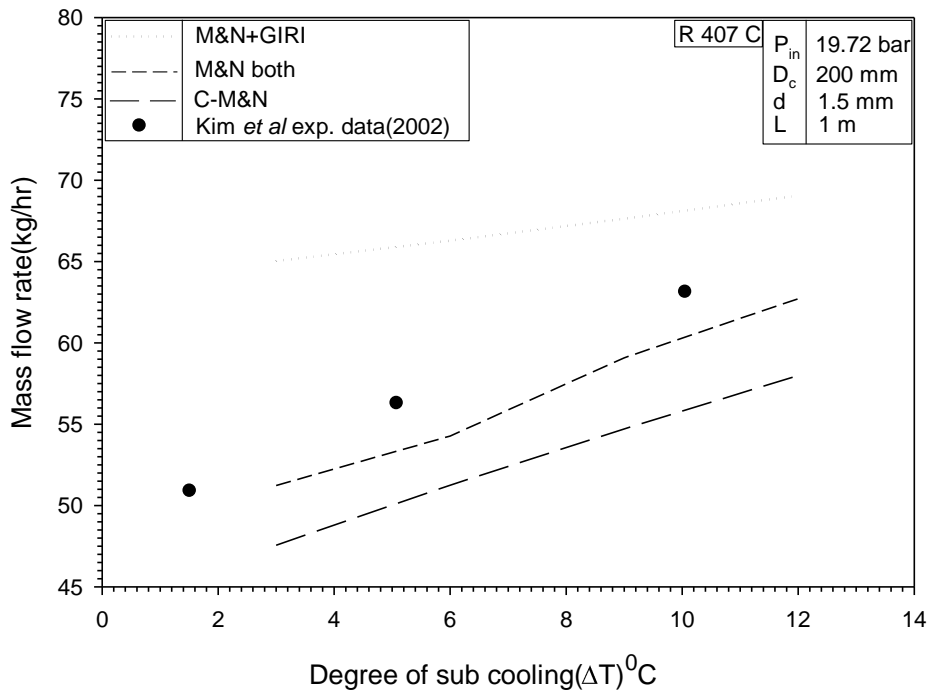


Fig.4.12: Comparison of Kim *et al.* (2002) experimental data with present numerical results at condenser pressure of 19.72 bar for the flow of R-407 C with coil diameter 200 mm.

4.1.7 Validation of mathematical model with Kim *et al.* (2002) experimental data for R-410 A with coil diameter 40,120,200 mm.

Fig.4.13, 4.14 and 4.15 shows comparison of Kim *et al.* (2002) experimental data with present models for condenser pressure of 14.7 bar. All three figures have been drawn shows that M&N equation shows the promising prediction for refrigerant R-410 A as compared to the other two equations to that of the experimental results by Kim *et al.* (2002). Mass flow rate of R-410 A also increased linearly like mass flow rate of R-407 C with increasing degree of sub cooling. Again it has been noted that M&N + GIRI over predicted mass flow rate compared to the experimental results. Helical capillary tube Length, coil diameter, evaporator pressure and tube diameter are 1 m, 40,120 and 200 mm, 5.22 bar and 1.5 mm respectively. Closest prediction is given by M&N equation for both single and two phase flow.

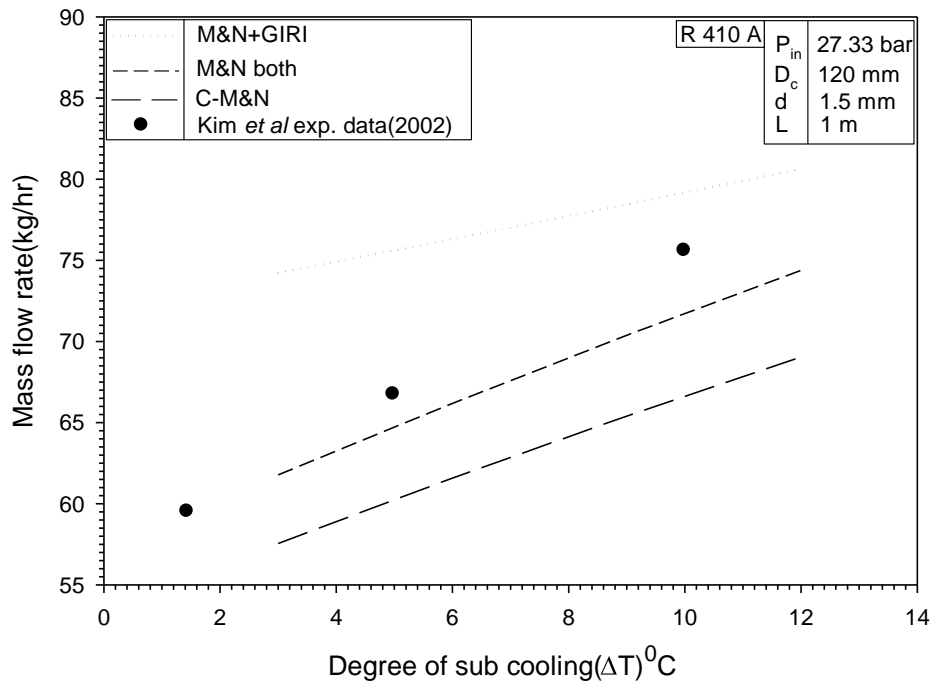
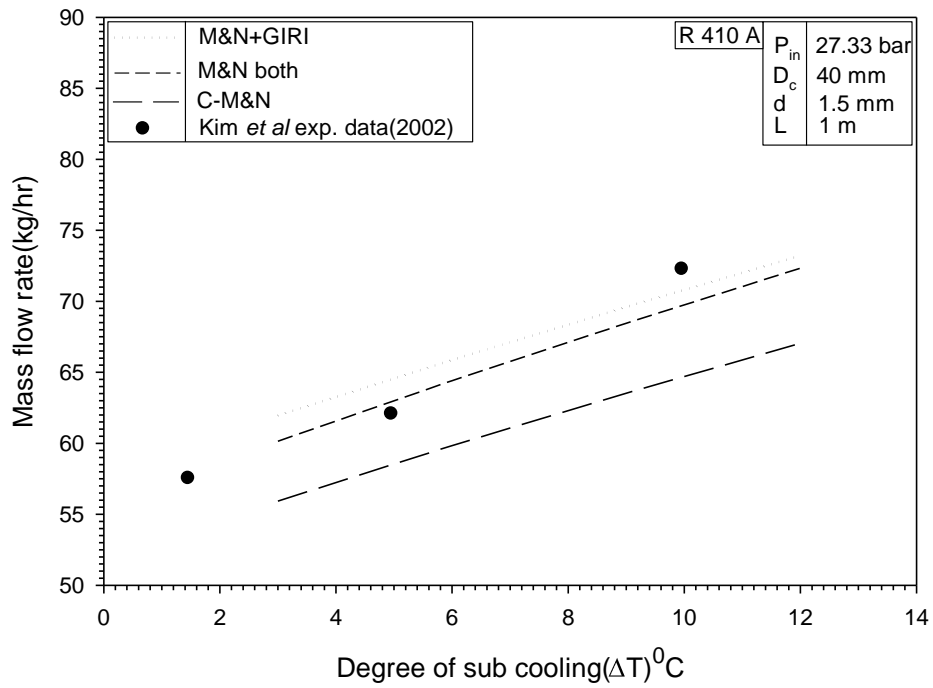


Fig.4.13 and 4.14: Comparison of Kim et al. (2002) experimental data with present numerical Result at condenser pressure of 27.33 bar for the flow of R-410 A with coil diameter 40 and 120 mm.

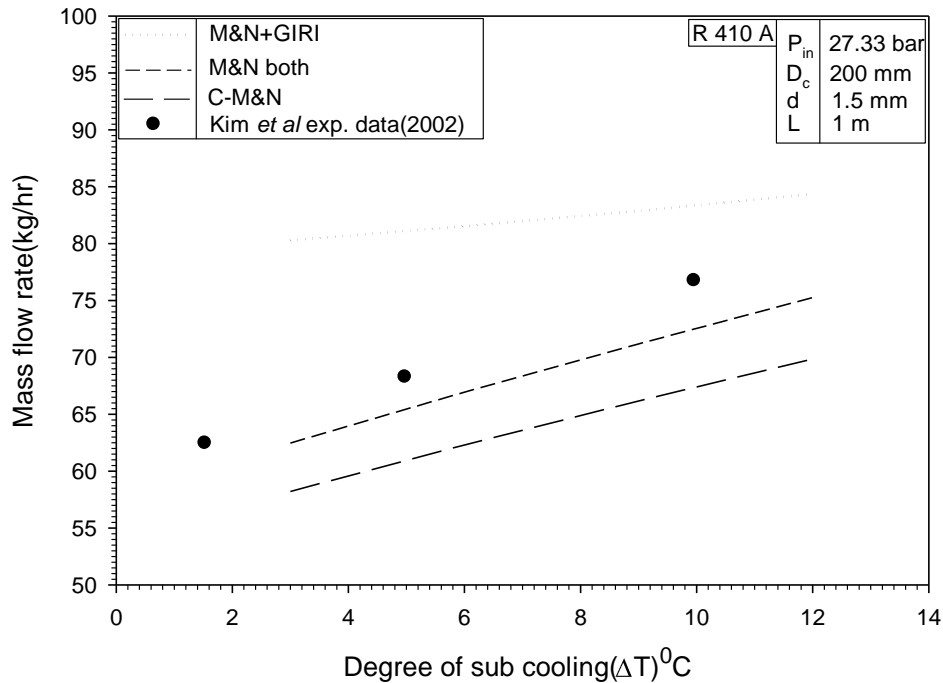


Fig.4.15: Comparison of Kim *et al.* (2002) experimental data with present numerical results at condenser pressure of 27.33 bar for the flow of R-410 A with coil diameter 200 mm.

4.1.8 Validation of mathematical model with Khan *et al.* (2008) experimental data for R-134a with coil diameter 40,120 and 200 mm.

Fig.4.16, 4.17 and 4.18 shows comparison of Khan *et al.* (2008) experimental data with present model results for condenser pressure of 7.23 bar. All three figures have been drawn shows that C-M&N equation shows the promising prediction for refrigerant R-134a as compared to the other two equations to that of the experimental results by Khan *et al.* (2008). Mass flows rate of R-134a also increased linearly as mass flow rate of R-407 C and R-410 A increased with increasing degree of sub cooling. Again it has been noted that M&N + GIRI over predicted mass flow rate compared to the experimental results. And mass flow rate given by C-M&N and M&N converge at a single point at higher mass flow rates. This is due to fact that mass flow rate gets choked at higher rate. Helical capillary tube Length, coil diameter, Evaporator pressure and tube diameter are 2.4 m, 140 mm, 6.22 bar and 1.4, 1.12 and 1.63 mm respectively.

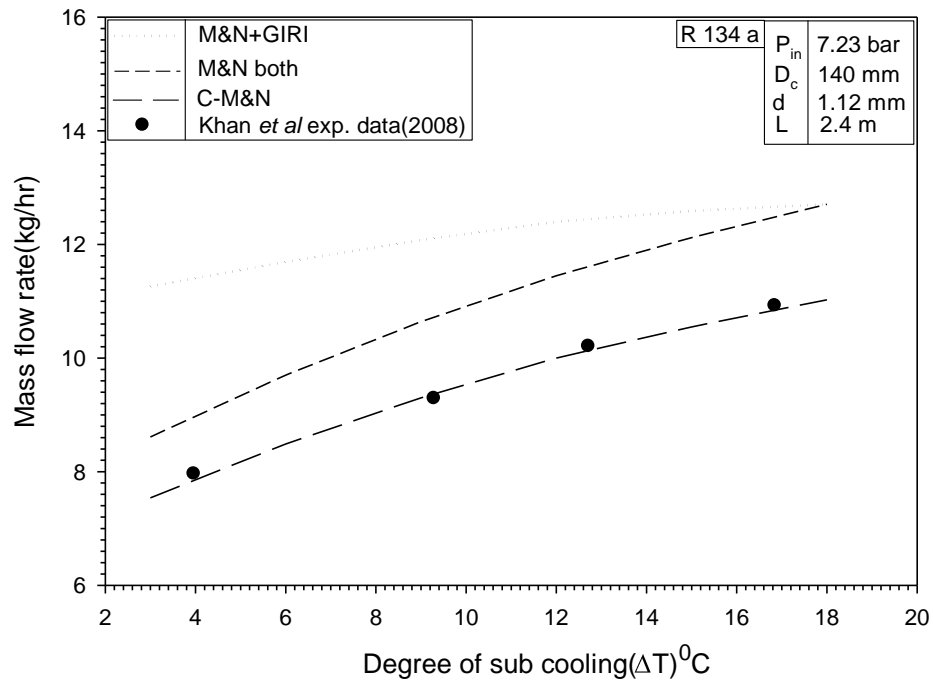
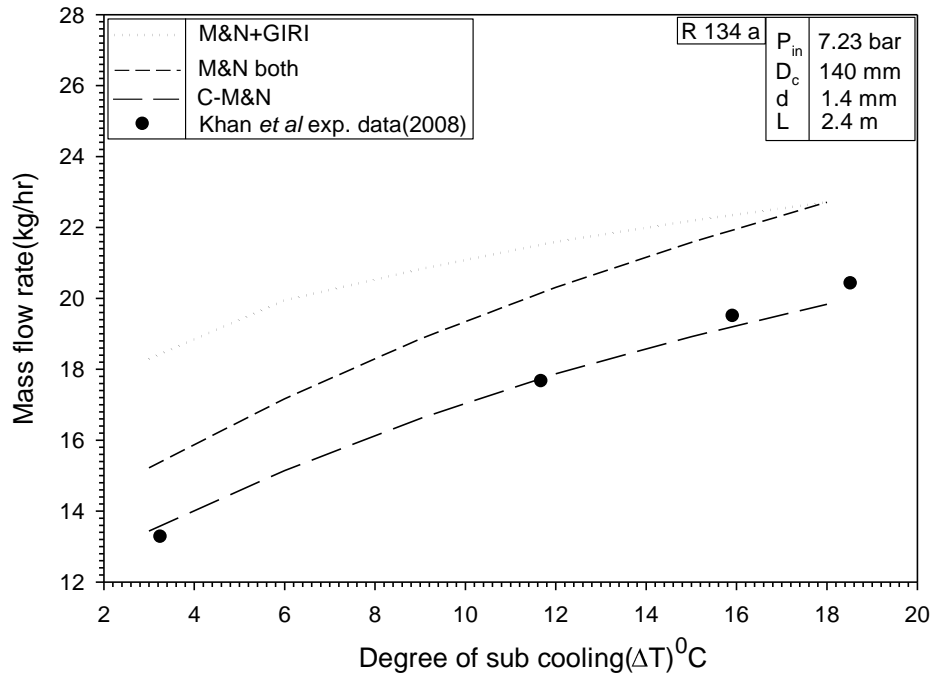


Fig.4.16, 4.17: Comparison of Khan et al. (2008) experimental data with present numerical results at condenser pressure of 7.23 bar for the flow of R-134a with coil dia 140 mm.

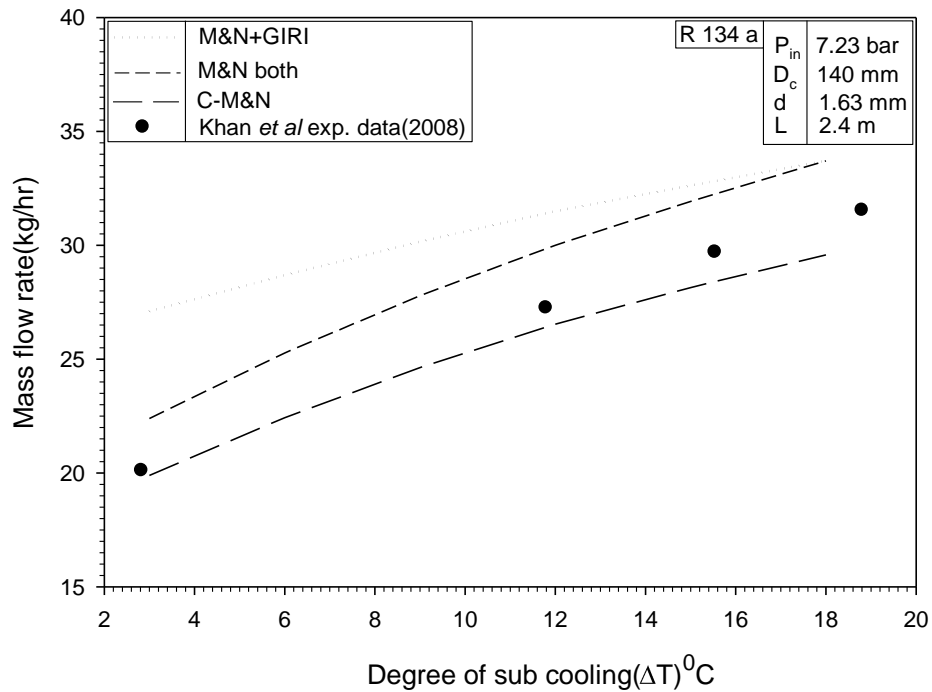


Fig.4.18: Comparison of Khan *et al.* (2008) experimental data with present numerical results at condenser pressure of 7.23 bar for the flow of R-134a with coil diameter 140 mm.

4.1.9 Validation of mathematical model with Khan *et al.* (2008) experimental data for R-134a with coil diameter 40,120,200 mm.

Fig.4.19, 4.20 and 4.21 shows comparison of Khan *et al.* (2008) experimental data with present simulated prediction for condenser pressure of 7.23 bar. All three figures have been drawn shows that C-M&N equation shows the promising prediction for refrigerant R-134a as compared to the other two equations to that of the experimental results by Khan *et al.* (2008). Mass flow rate of R-134a also increased linearly like mass flow rate of R-407 C and R-410 A with increasing degree of sub cooling. Again it has been noted that M&N + GIRI over predicted mass flow rate compared to the experimental results. And mass flow rate given by C-M&N and M&N converge at a single point at higher mass flow rates. Helical capillary tube Length, coil diameter, Evaporator pressure and tube diameter are 3.2 m, 140 mm, 6.22 bar and 1.4, 1.12 and 1.63 mm respectively.

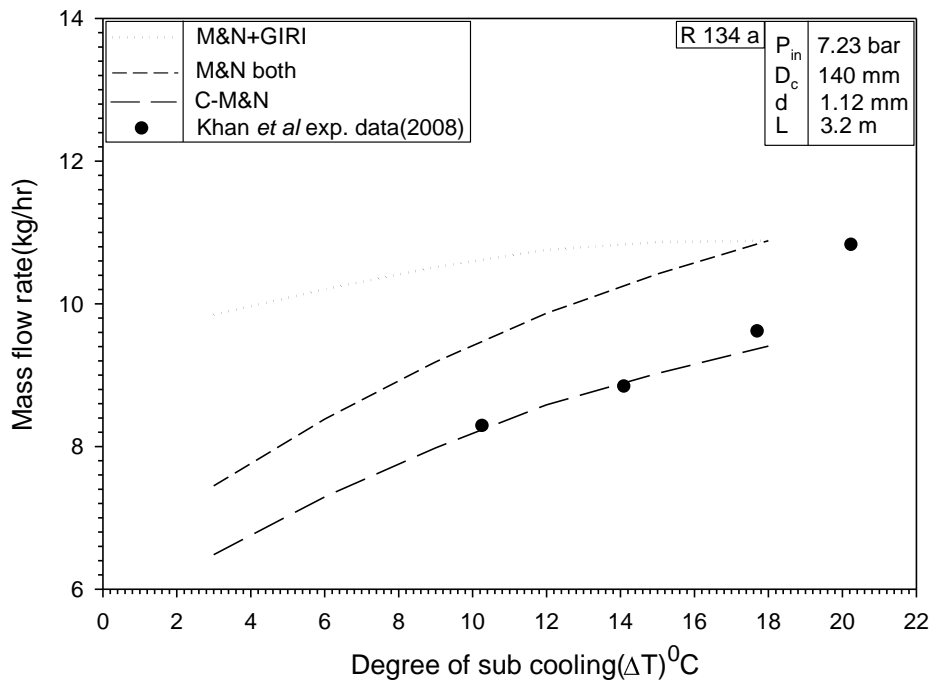
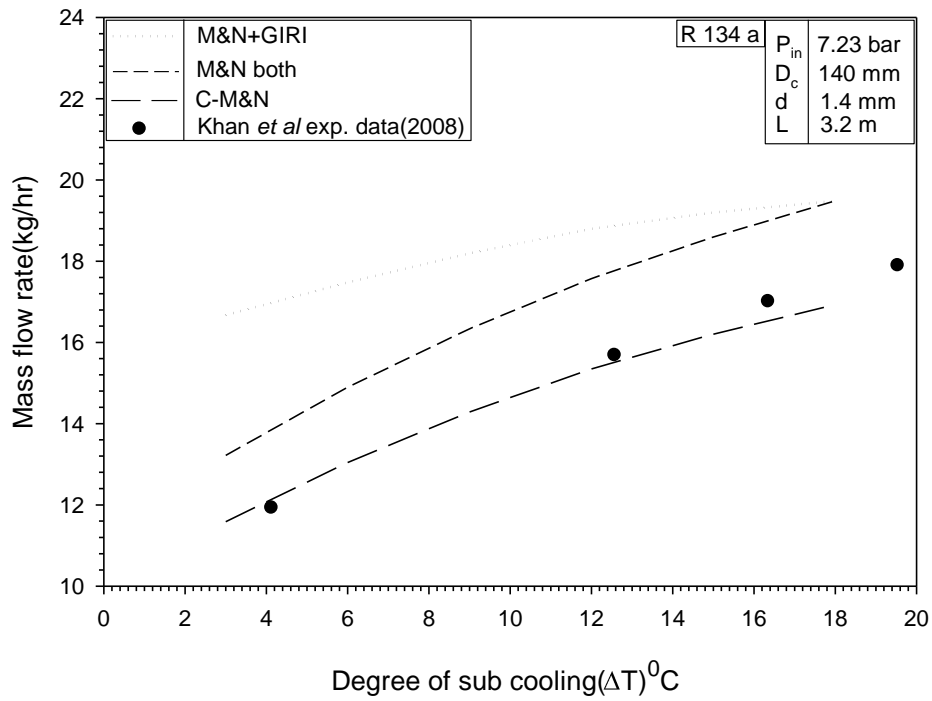


Fig.4.19 and 4.20: Comparison of Khan et al. (2008) experimental data with present numerical results at condenser pressure of 7.23 bar for the flow of R-134a with coil diameter 140 mm.

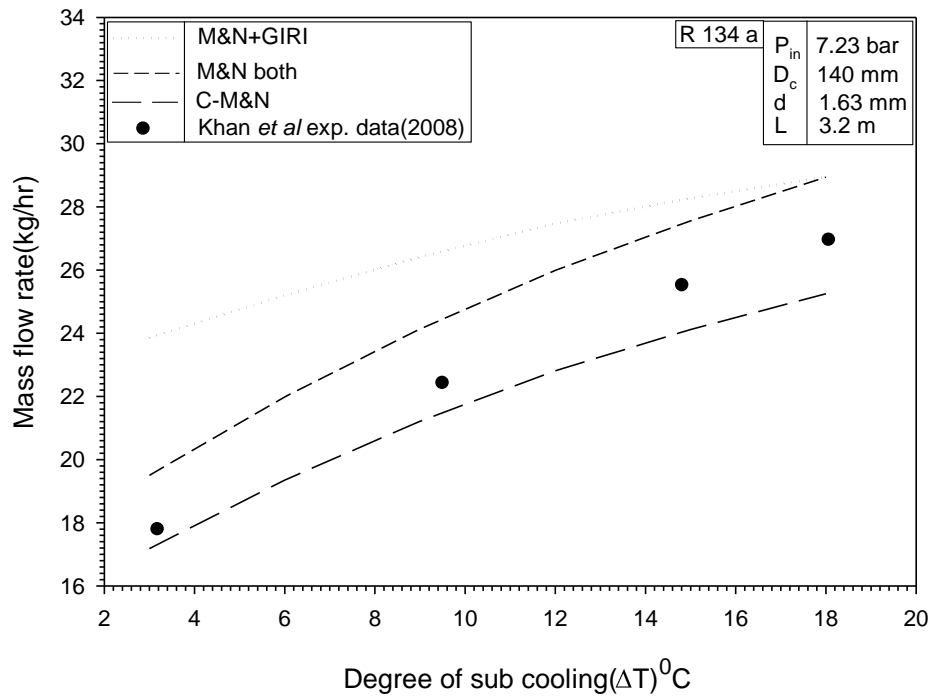


Fig.4.21: Comparison of Khan *et al.* (2008) experimental data with present numerical results at condenser pressure of 7.23 bar for the flow of R-134a with coil diameter 140 mm.

Fig.4.22 shows comparison of Mittal *et al.*(2009) and Kim *et al.*(2008) measured mass flow rate with predicted mass flow rate deviation (%) using all three equation M&N, C-M&N and M&N + GIRI. M&N equation gives us the best result with a deviation only $\pm 5\%$ for refrigerant R 407 C. However only viscosity model used is duklers viscosity model. Every time for R 407 C M&N+GIRI overestimates the mass flow rate and C-M&N equation under estimate the mass flow rate. M&N+GIRI equation gives the maximum upper deviation in mass flow rate is $+22\%$. And the minimum mass flow rate deviation is given by C-M&N equation which is -13% . It is clear from the figure that maximum predicted mass flow rate prediction given by M&N equation lays very close to zero line for R407C.

Similarly Fig. 4.23 and 4.24 comparison of measured and predicted mass flow rate deviation. In Fig. 4.23 measured data on y-axis extracted from Kim *et al* (2002) for refrigerant R 410 A. M&N equation gives us the best result and give a deviation only $\pm 7\%$ for refrigerant R 410 A.

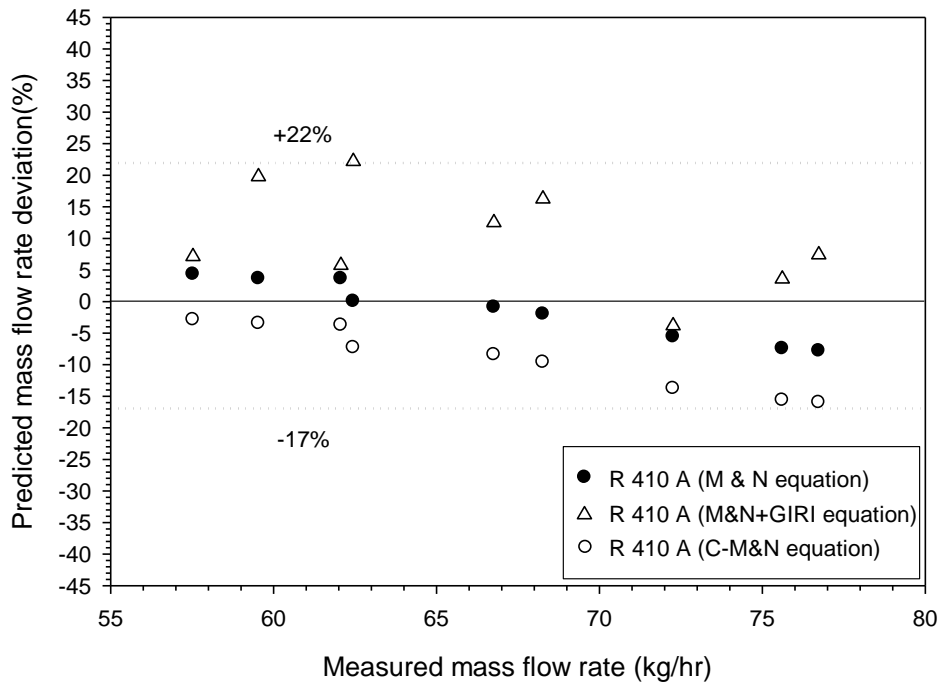
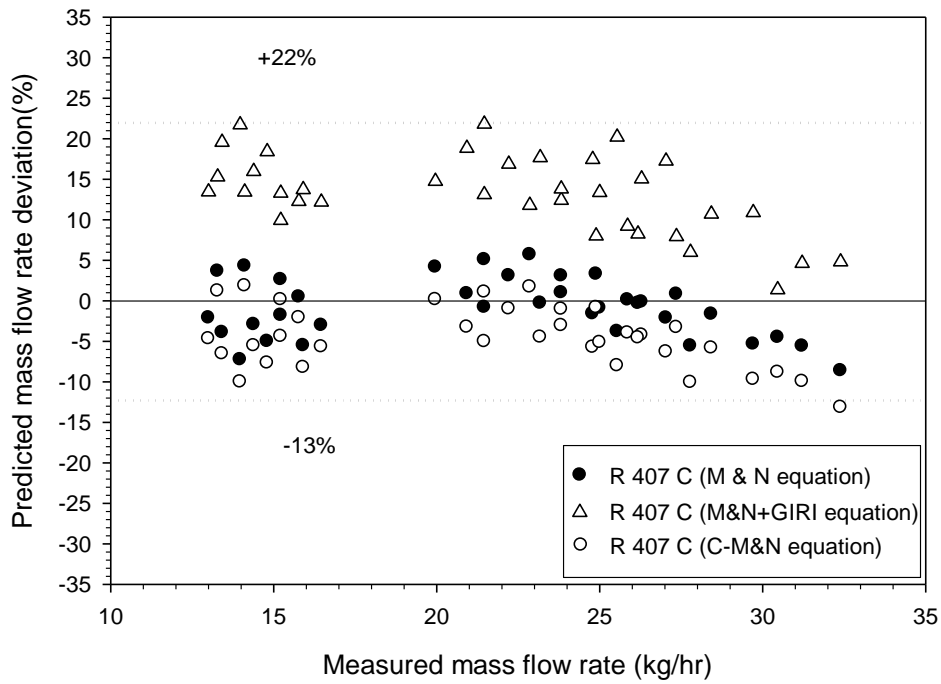


Fig.4.22 and 4.23: Comparison of measured mass flow rate and predicted mass flow rate deviation of refrigerant R-407 C and R-410 A using M&N, M&N+GIRI and C-M&N equations.

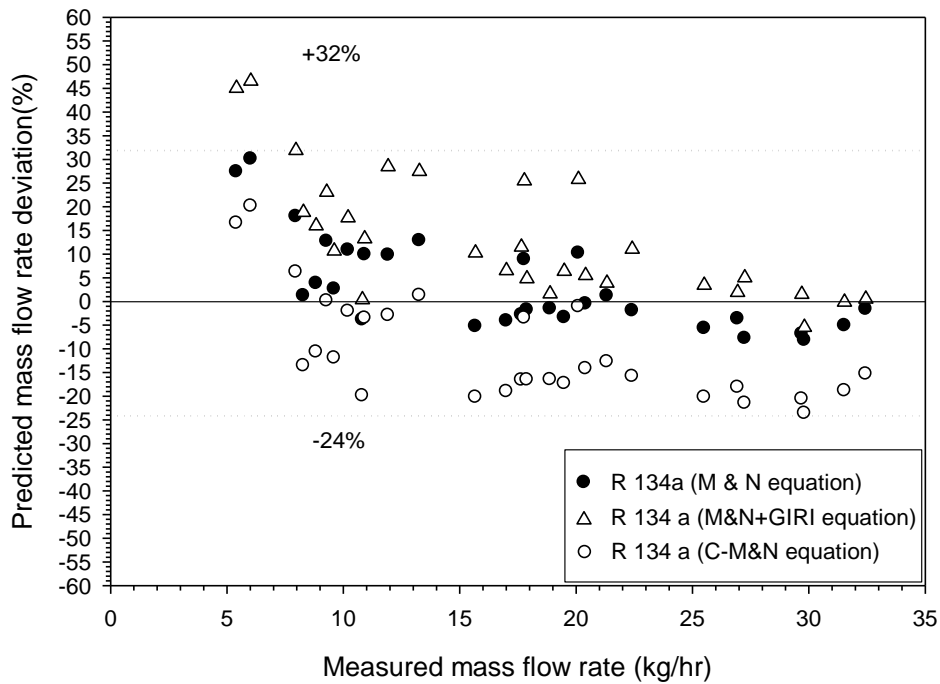
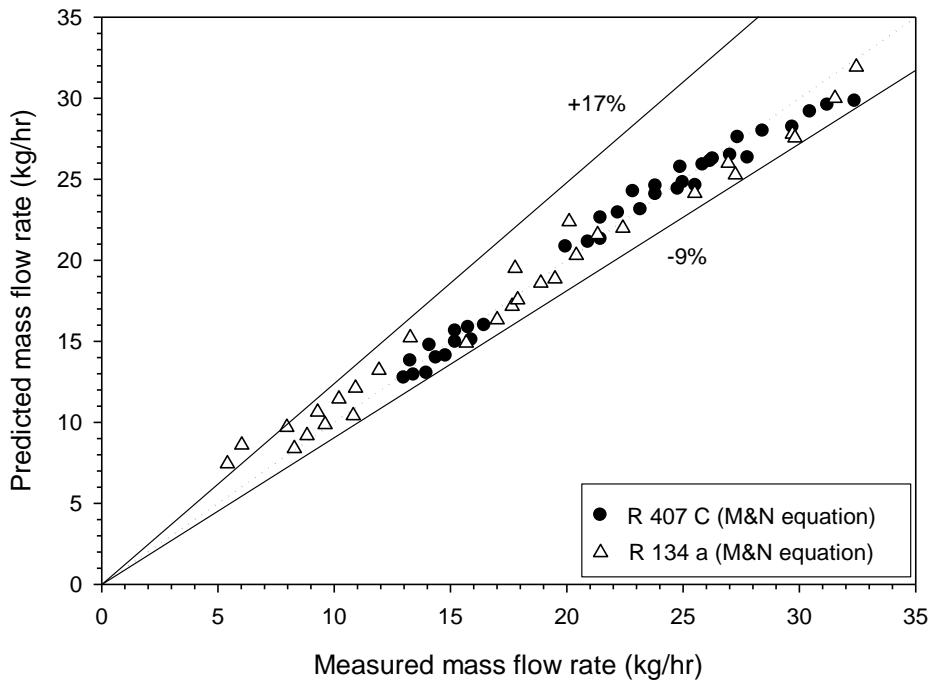


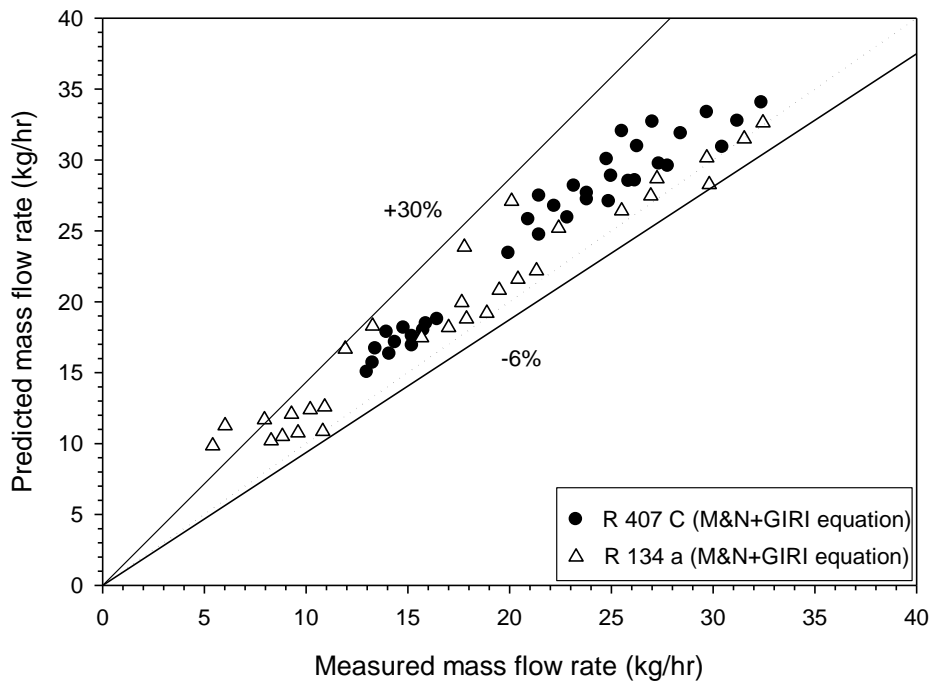
Fig.4.24: Comparison of measured mass flow rate and predicted mass flow rate deviation of refrigerant R-134a using M&N, M&N+GIRI and C-M&N equation.

M&N+GIRI overestimate the mass flow rate and C-M&N equation under estimate the mass flow rate. M&N+GIRI equation gives the maximum upper deviation in mass flow rate is +22 %. And the minimum mass flow rate deviation is given by C-M&N equation which is -17 %. In fig, 4.24 measured data on y-axis extracted from Khan *et al* (2008) for refrigerant R 134 A. M&N equation gives us the best result and give a deviation ± 15 % for refrigerant R 134a. M&N+GIRI equation gives the maximum upper deviation in mass flow rate is +32 %. And the minimum mass flow rate deviation is given by C-M&N equation which is -24 %.

Fig.4.25 a, b and c shows the comparison of experimental mass flow rates of Mittal *et al.* (2009) and Khan *et al* (2008) with the numerical mass flow rates predicted by the proposed model. It is observed that 90 percent experimental data of refrigerants R-134a and R-407 C falls in the region of predicted data while using M&N equation for both single and two phase flow of refrigerant. Standard deviation for M&N equation lies from -9 % to +17 %. And values for M&N+GIRI and C-M&N are -6% to +32% and -24% to +21% respectively.



(a)



(b)

Fig.4.25 (a and b): Comparison of measured mass flow rate with predicted mass flow rate for refrigerant R-134a and R-407 C.

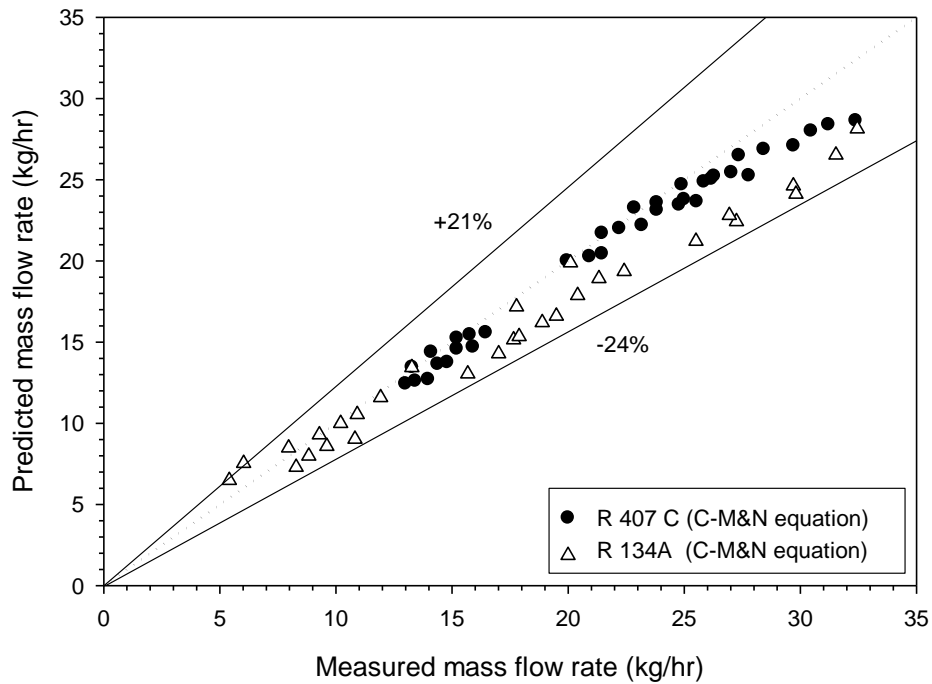


Fig.4.25 (c): Comparison of measured mass flow rate with predicted mass flow rate for refrigerants R-134a and R-407 C.

4.2 Simulation of refrigerants R-407 C, R-410 A, R134a, R-12 and R-404 A using M&N equation for both single and two phase length.

Since refrigerant R-22 has ozone depletion potential, its use is being stopped in the phase manner. The use of refrigerant R-22 is being phased out. From January 1, 2010 there would be complete ban on the production and import of R-22 though it will be allowed for the servicing for the existing refrigeration equipment. Eventually, by January 1, 2020, there would be complete ban on the refrigerant. Here we have simulation results on alternative of R-22 which are R-407 C, R-410 A and R-404 A. We also have simulation results of refrigerant R-12 and its alternative R-134a which is only available alternative for the refrigerant. Refrigerant R-407 C, R-410 A and R-404 A are the mixture or blends of the different refrigerants in various proportions. R-407 C is a mixture of R-32 (.23), R-125 (.25) and R-134a (.52). Similarly R-410 A is a mixture of R-32 (0.5) and R-125 (0.5) and R-404 A is a mixture of R-125 (.44), R-143a (.52) and R-134a (.04).

4.2.1 Simulation results of refrigerants R-407 C, R-410 A, R134a, R-12 and R-404 A using M&N equation for effect of sub cooling on mass flow rate.

Fig.4.26 have been drawn to show the simulated results of refrigerant R-407 C, R-410 A, R134a, R-12 and R-404 A. It has been observed that mass flow rate increases with increased degree of sub cooling at inlet. We previously observed the same phenomenon while validating the model results with experimental results. It can also be observed that mass flow rate of R-407 C and R-404 A are very close to each other as both are the alternative of refrigerant R-22. However mass flow rate of R-410 A are slightly higher than the other two alternatives. It has also been observed from the figure that R-12 and its alternative R-134a almost have same mass flow rate of given degree of sub cooling. Helical capillary tube Length, coil diameter, Evaporator pressure and tube diameter are 2 m, 60 mm, 4.22 bar and 1.27 mm respectively.

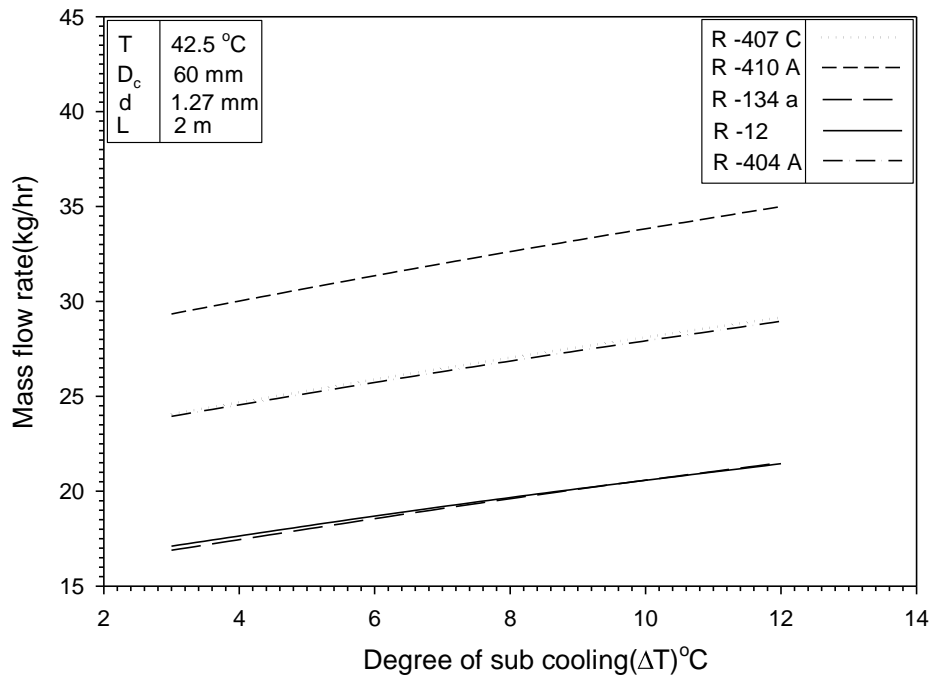


Fig.4.26: Mass flow rate variation with degree of sub cooling for refrigerants R-407 C, R-410 A, R134a, R-12 and R-404 A for lengths of 2 m and 1.27 mm tube diameter with condenser temperature of 42.5°C.

Fig.4.27 and 4.28 have been drawn to show the simulated results of refrigerant R-407 C, R-410 A, R134a, R-12 and R-404 A. Mass flow rate increases with degree of sub cooling observed the

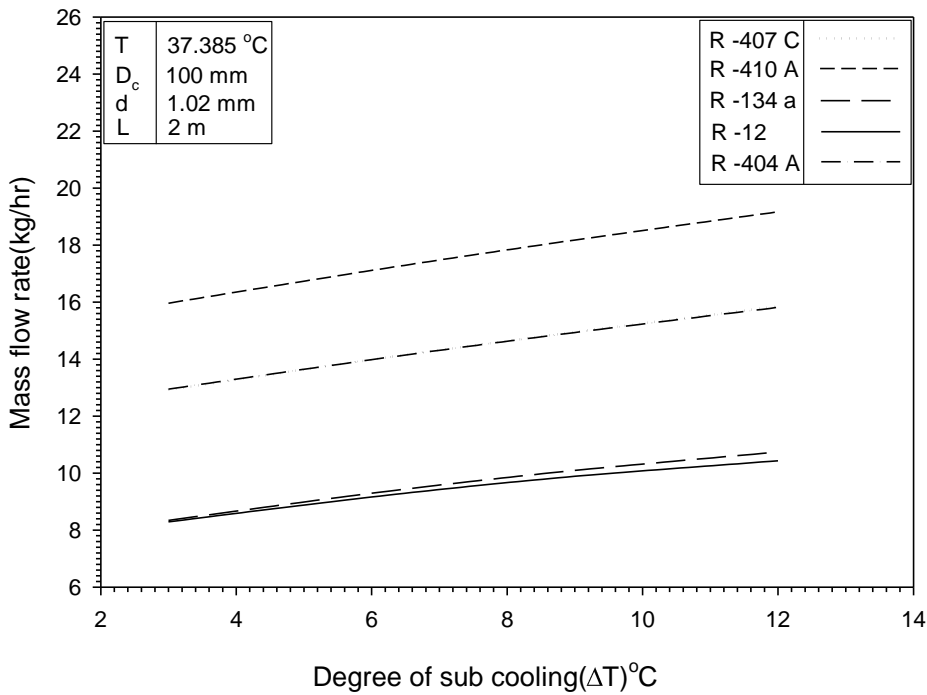
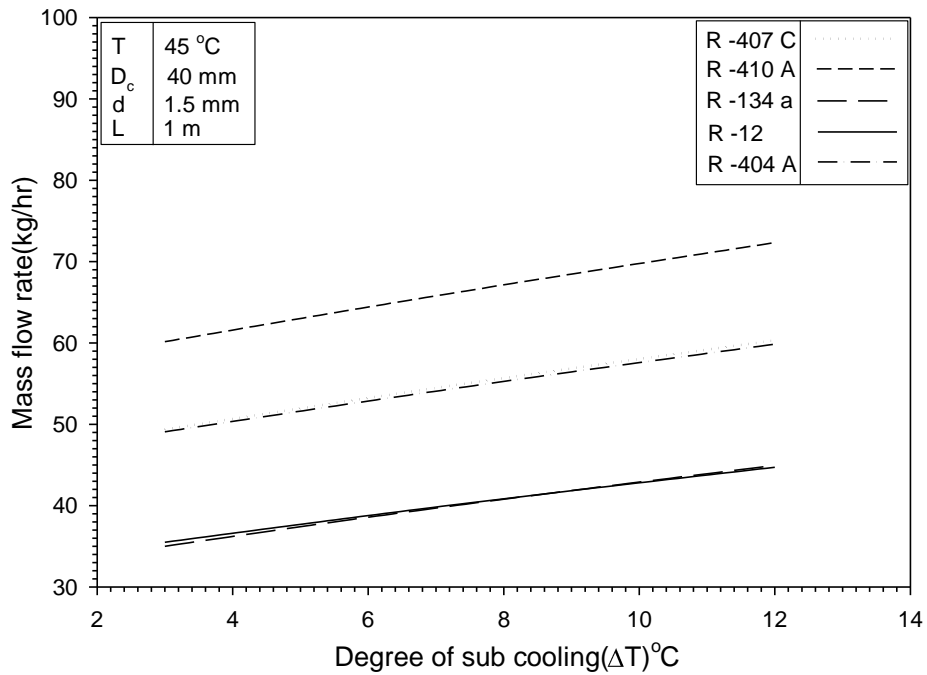


Fig.4.27 and 4.28: Mass flow rate variation with degree of sub cooling for refrigerants R-407 C, R-410 A, R134a and R-404 A for lengths of 1m, 2 m and 1.27, 1.02 mm tube diameter and condenser temperature of 45 and 37.38 $^{\circ}\text{C}$.

phenomenon while validating the model results with experimental results. It can also be observed from both the figures that mass flow rate of R-407 C and R-404 A are very close to each other as both are the alternative of refrigerant R-22. However mass flow rate of R-410 A are slightly higher than the other two alternatives. It has also been observed from both the figures that R-12 and its alternative R-134a almost have same mass flow rate of given degree of sub cooling. Helical capillary tube Length, coil diameter, Evaporator pressure and tube diameter are 1, 2 m, 40, 100 mm, 4.22 bar and 1.6, 1.02 mm respectively.

4.2.2 Simulation results of refrigerants R-407 C, R-410 A, R134a, R-12 and R-404 A using M&N equation for effect of coil diameter on mass flow rate.

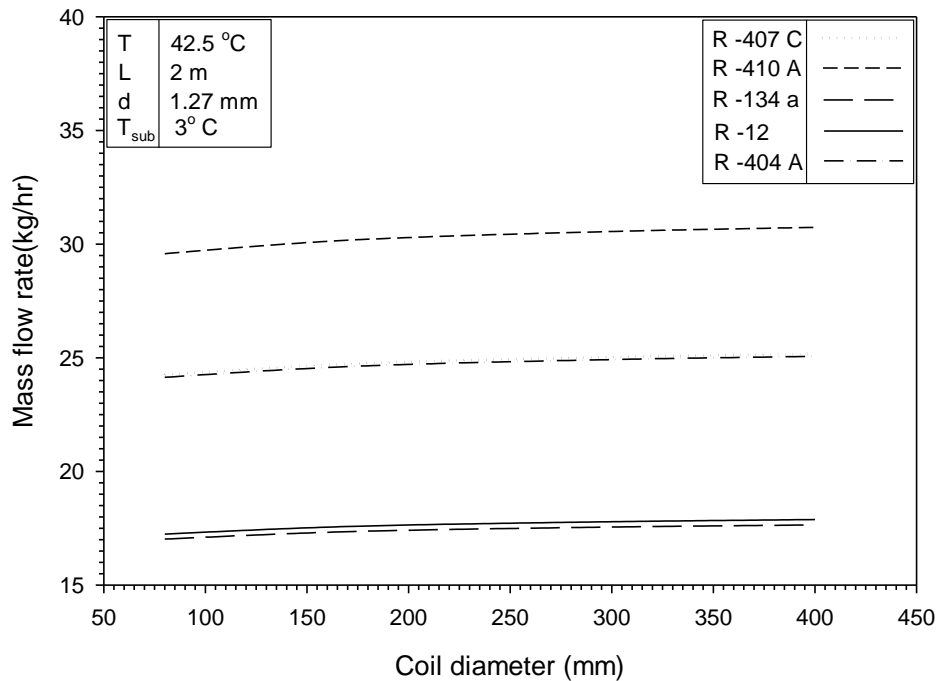


Fig.4.29: Mass flow rate variation with coil diameter for refrigerants R-407 C, R-410 A, R134a, R-12 and R-404 A for lengths of 2 m and 1.27 mm tube diameter, sub cooling 3° C and condenser temperature of 42.5° C.

Fig 4.29 has been drawn to show the effect of increasing helical capillary tube diameter on mass flow rate of refrigerant. It already has been known that helical capillary has higher mass flow rate as compared to straight capillary tube due to secondary flow in helical capillary tube. But as

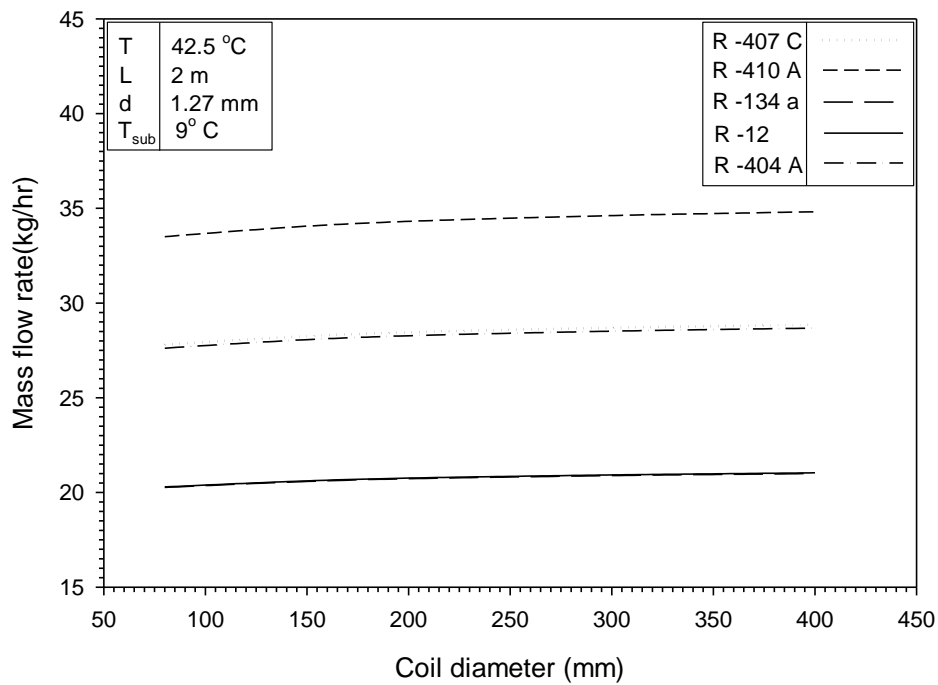
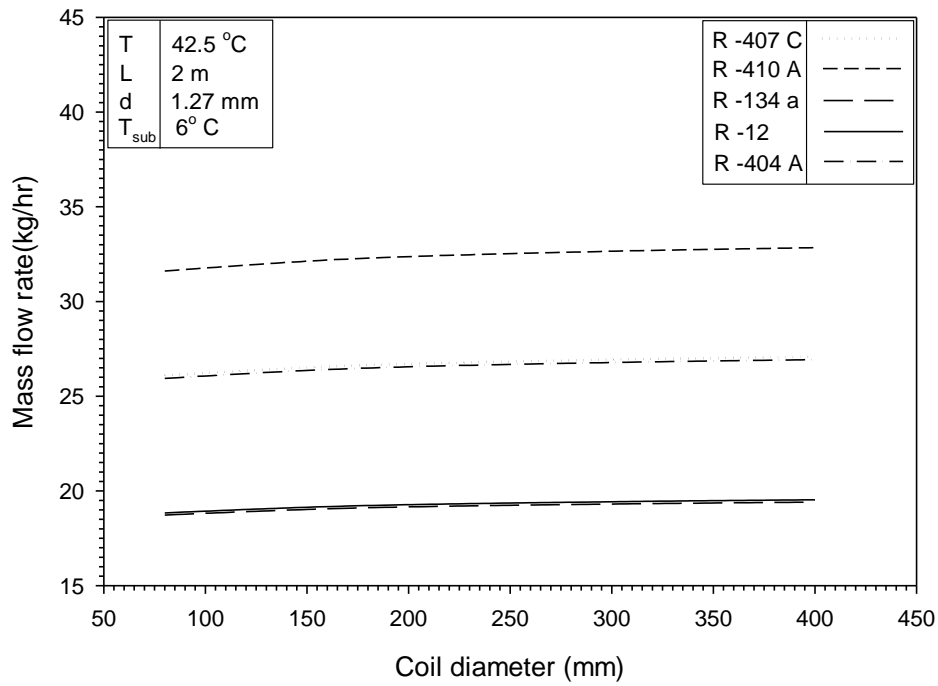


Fig.4.30, 4.31: Mass flow rate variation with coil diameter for refrigerants R-407 C, R-410 A R134a, R-12 and R-404 A for lengths of 2 m and 1.27 mm tube diameter, sub cooling 6,9°C, and condenser temperature of 42.5°C.

shown in fig 4.29 change in coil diameter has very little effect on mass flow rate of refrigerant. The lines with increasing coil diameter go horizontally straighter. Similarly figures 4.30 and 4.31 have been drawn between mass flow rate and coil diameter with different degree of sub cooling. There is a very minor increase in mass flow rate observed while increasing helical capillary tube coil diameter.

4.2.3 Simulation results of refrigerants R-407 C, R-410 A, R134a, R-12 and R-404 A using M&N equation for effect of evaporator pressure on mass flow rate.

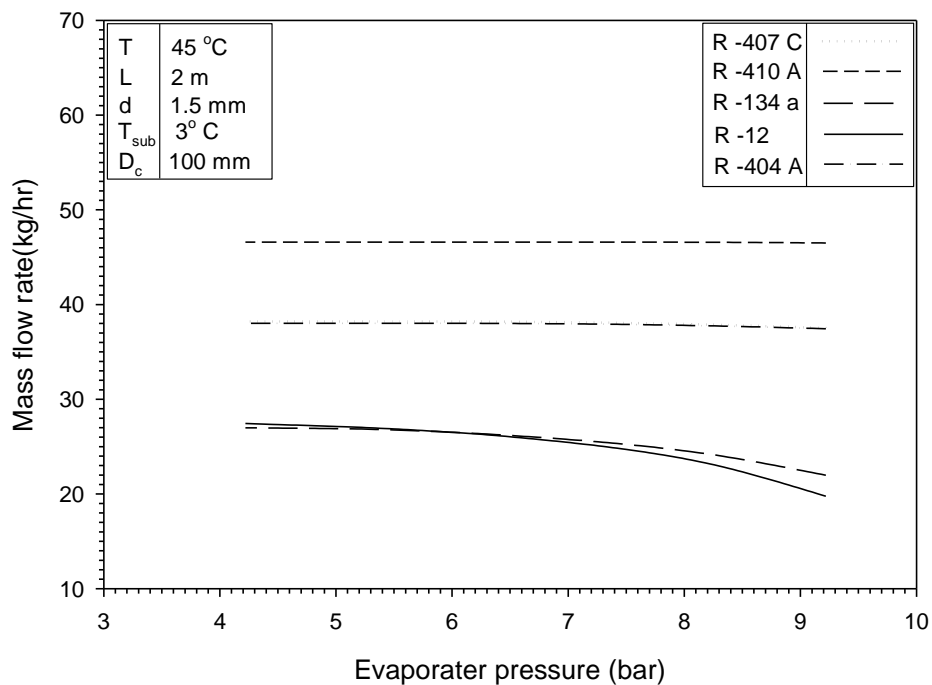


Fig.4.32: Mass flow rate variation with evaporator pressure for refrigerants R-407 C, R-410 A, R134a, R-12 and R-404 A for lengths of 2 m and 1.5 mm tube diameter, sub cooling 3° C and condenser temperature of 45° C.

Fig 4.32 has been drawn to show the effect of increasing evaporator pressure on mass flow rate of refrigerant. It is clear from the drawn figure that the mass flow rate increases with decrease in evaporator pressure and decreases with increasing evaporator pressure. In case of refrigerant R-12 and R-134a there is a notable increase in mass flow rate of these refrigerants while in case of

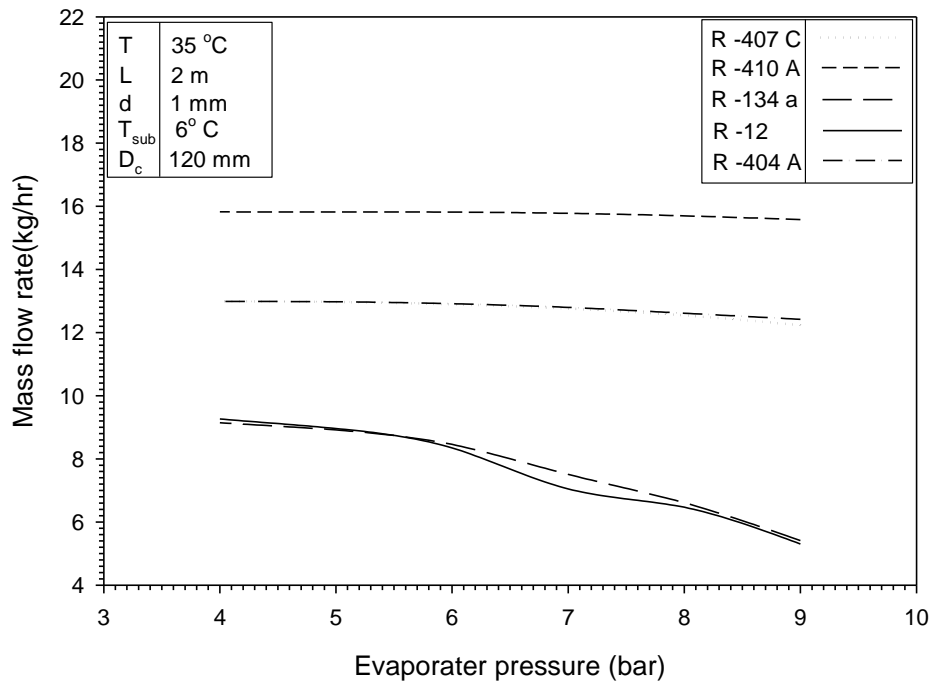
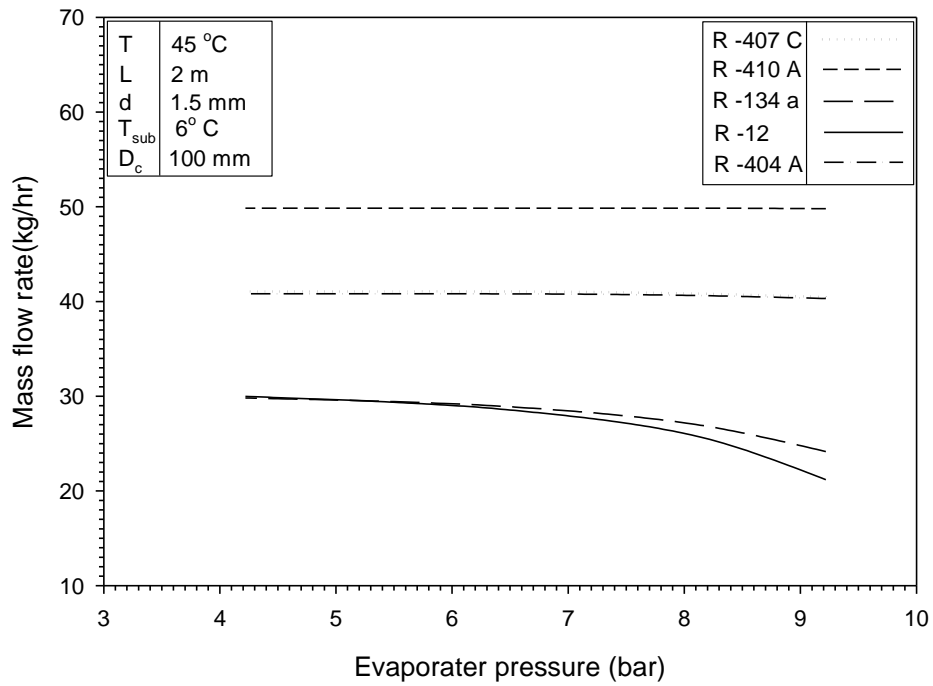


Fig.4.33 and 4.34: Mass flow rate variation with evaporator pressure for refrigerants R-407 C, R-410 a, R134a, R-12 and R-404 a for lengths of 2 m and 1.5 m, 1 mm tube diameter, sub cooling 6°C and condenser temperature of 45 and 35°C.

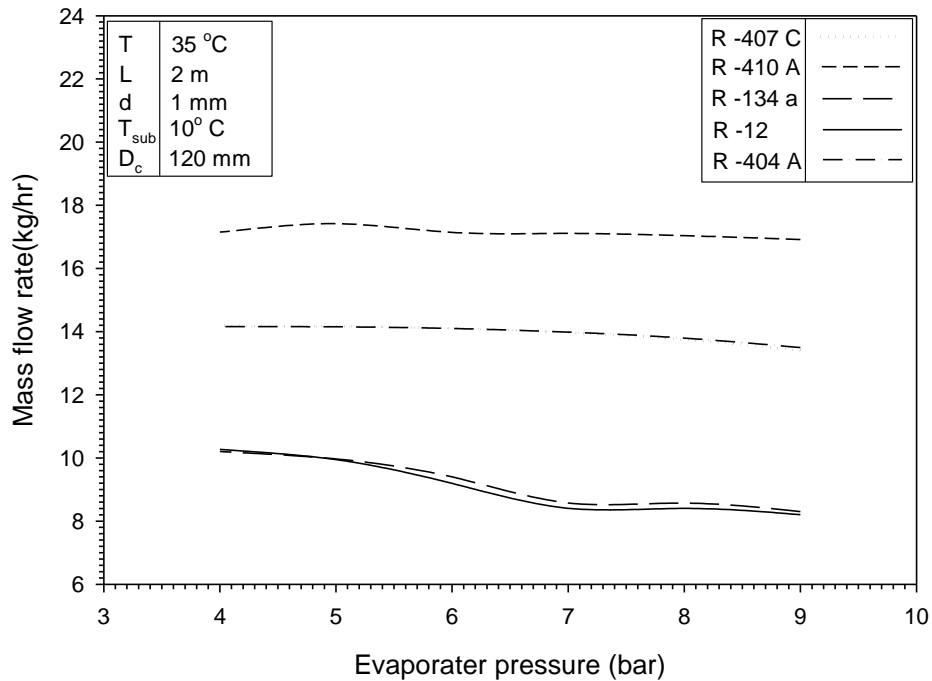


Fig.4.35: Mass flow rate variation with evaporator pressure for refrigerants R-407 C, R-410 A, R134a, R-12 and R-404 A for lengths of 2 m and 1 mm tube diameter, sub cooling 10°C and condenser temperature of 35°C.

other three refrigerants R-407 C, R-404 and R-410 A lines are straighter and not so much deflected while decreasing evaporator pressure. Similarly Fig 4.33 has been drawn to show the effect of increasing evaporator pressure on mass flow rate of refrigerant. It is observed from the drawn figure that the mass flow rate increases with decrease in evaporator pressure and decreases with increasing evaporator pressure. R-12 and R-134a shows a wavy character while mass flow rate of evaporator decreases. There are also some slight up and down in other three refrigerant in figure 4.34 and 4.35.

4.2.4 Simulation results of refrigerants R-407 C, R-410 A, R134a, R-12 and R-404 A using M&N equation for effect of capillary tube diameter on mass flow rate.

Fig 4.36, 4.37 has been drawn to show the effect of capillary tube diameter on capillary tube mass flow rate. It has been observed that the mass flow rate increases tremendously with increase in capillary tube diameter. R-410 A give the maximum mass flow rate in given conditions. R-12 and R-134a follows almost the same path. On the other side R-407 and R-404 A follows the same path. All these values are taken for 3°C sub cooling. Condenser temperature, coil diameter

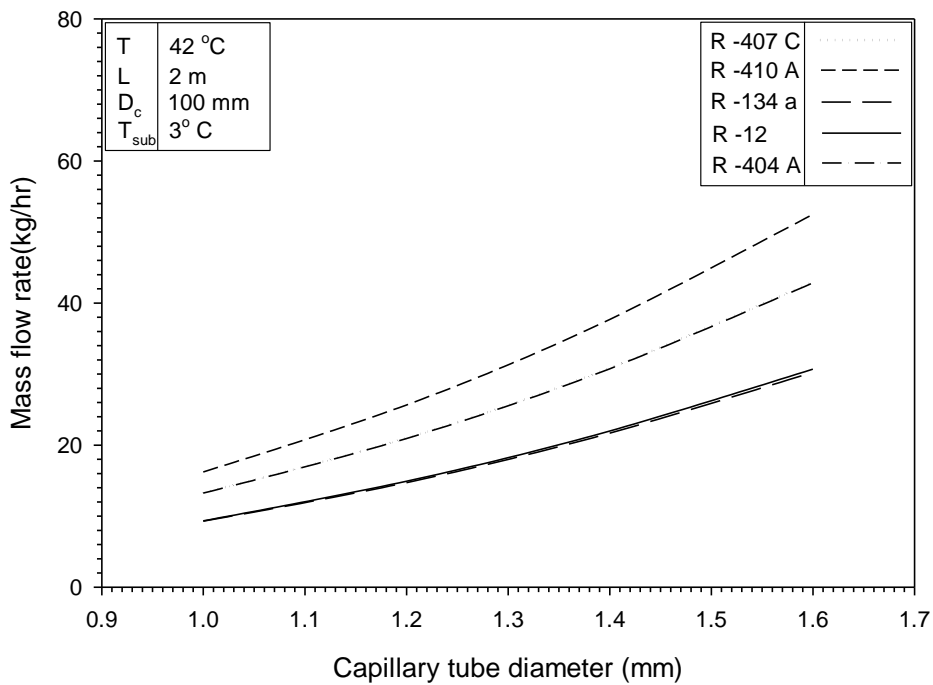
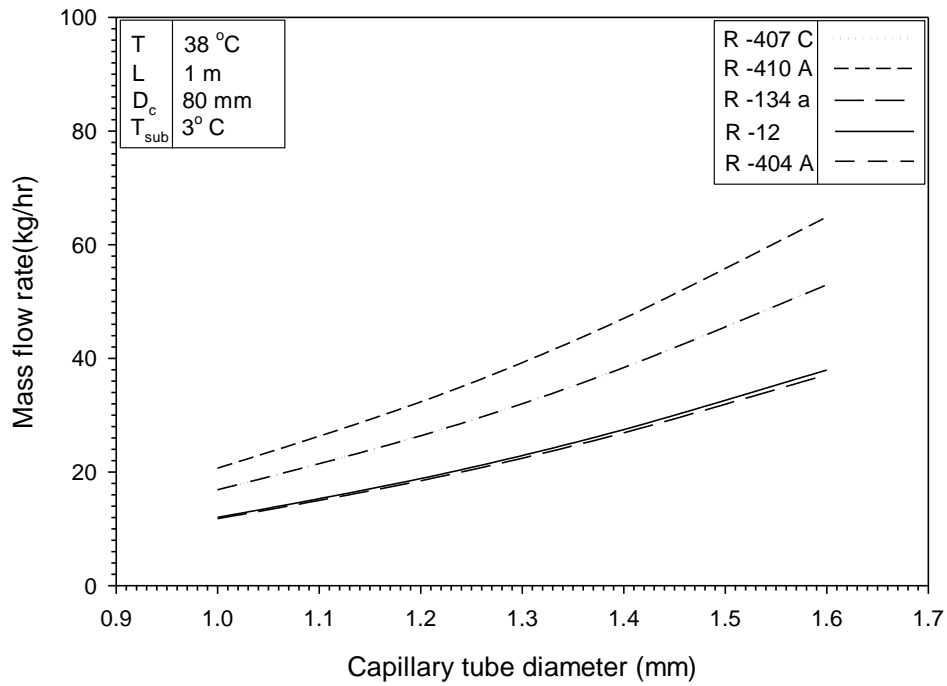


Fig.4.36 and 4.37: Mass flow rate variation with capillary tube diameter for refrigerants R-407 C, R-410 A, R134a, R-12 and R-404 A for lengths of 1,2 m, coil diameter 80,100 mm, sub cooling 3°C and condenser temperature of 38 and 42°C.

and length of capillary tube are 38°C, 80 mm and 1 m respectively. It has also been observed that the conditions for figure 4.36 and 4.37 are different but the trends followed by the lines are almost same.

4.2.5 Simulation results of refrigerants R-407 C, R-410 A, R134a, R-12 and R-404 A using M&N equation for effect of capillary tube inlet pressure on mass flow rate.

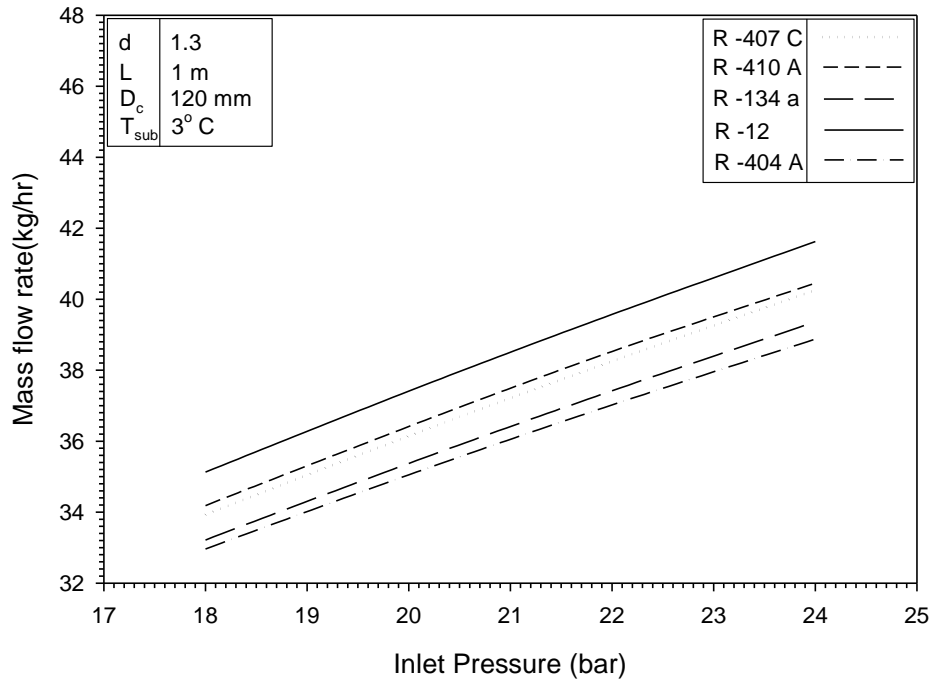


Fig.4.38: Mass flow rate variation with inlet pressure for refrigerants R-407 C, R-410 A, R134a, R-12 and R-404 A for lengths of 1 m and 1.3 mm tube diameter, sub cooling 3°C and coil diameter 120 mm.

Fig. 4.38 shows the effect of capillary tube inlet pressure on mass flow rate. It has been observed that there is a linear increase of mass flow rate with increase in capillary tube inlet pressure. Every refrigerant have almost different trend line according to different inlet pressure. However R-407 and R-410 and R-134a and R-404 have close approximation. Similarly in fig. 4.39 with capillary diameter 1.6 and coil diameter 140 mm it has been observed that mass flow rate varies linearly with the increasing inlet pressure.

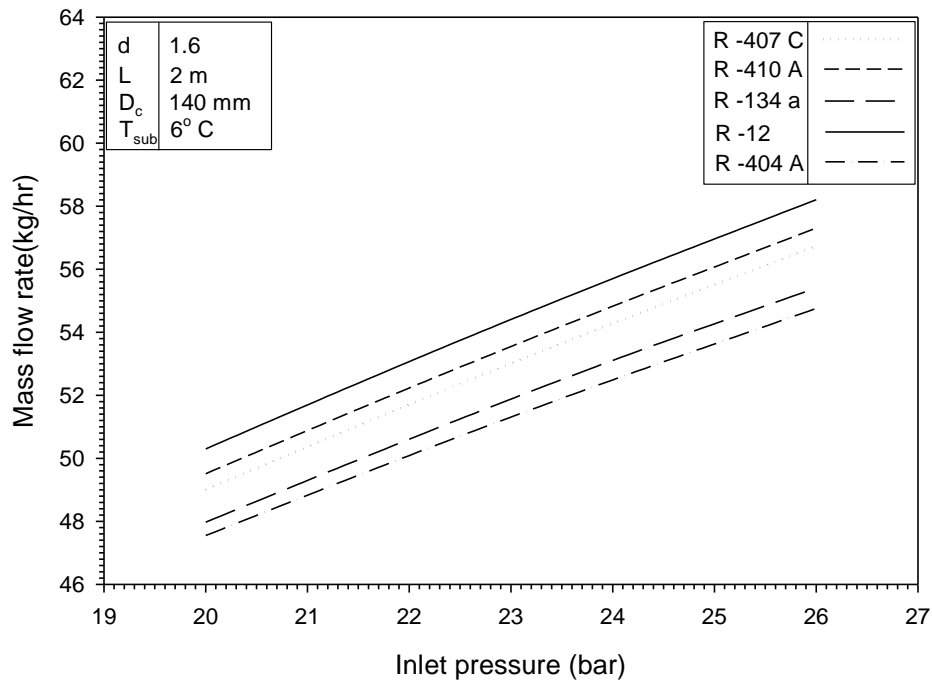


Fig.4.39: Mass flow rate variation with inlet pressure for refrigerants R-407 C, R-410 A, R134a, R-12 and R-404 A for lengths of 2 m and 1.6 mm tube diameter, sub cooling 6°C and coil diameter 140 mm.

4.2.6 Variation of pressure of refrigerants R-407 C, R-410 A, R134a, R-12 and R-404 A along a capillary tube length.

Fig.4.40 has been drawn to show the pressure variation of different refrigerant flowing through the capillary tube length. It has been observed that there is a linear pressure variation in single phase. And pressure drop is more rapid and non linear in two phase flow. A constant mass flow rate of 28 kg/hr has been maintained for all five refrigerants. It has been also been observed that R-404 A has greater pressure drop in all within shorter length span among all refrigerants. And on the other hand R-12 requires longest length in all refrigerants taken for study. While all other refrigerant are within the R-12 and R-404 A. However R-407 C also has a good agreement in between the R-12 and R-404 A. Condenser pressure, coil diameter and diameter of capillary tube are 22 bar , 60 mm and 1.15 mm respectively.

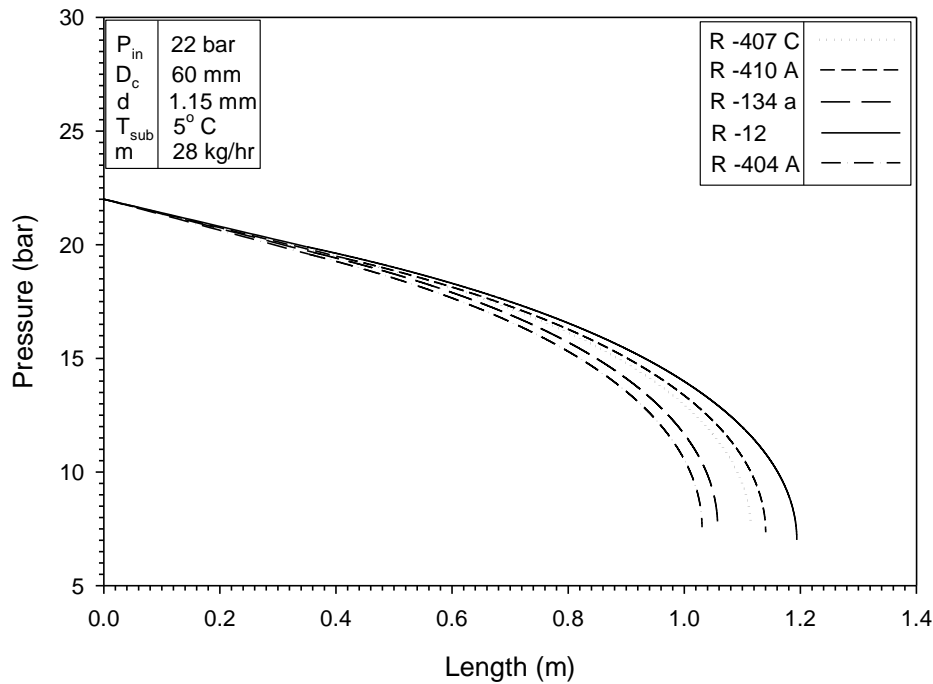


Fig.4.40: Variation of pressure for refrigerants R-407 C, R-410 A, R134a, R-12 and R-404 A along a capillary tube length for pressure 22 bar, 1.15 mm tube diameter, sub cooling 5° C and coil diameter 60 mm.

4.2.7 Variation of temperature of refrigerants R-407 C, R-410 A, R134a, R-12 and R-404 A along a capillary tube length.

Fig.4.41 has been drawn to show the temperature variation of different refrigerant flowing through the capillary tube length. It has been observed that there constant temperature in single phase. This is due to fact that capillary tube is adiabatic. And temperature drop is more rapid and non linear in two phase flow. A constant mass flow rate of 22 kg/hr has been maintained for all five refrigerants. It has been also been observed that R-12 has greater temperature drop in all within shorter length span among all refrigerants. And on the other hand R-410 A requires longest length in all refrigerants taken for study. While all other refrigerant are within the R-12C and R-410 A. However R-407 C and R-404 A also has a good agreement in between the R-12 and R-404 A. Condenser temperature, coil diameter and diameter of capillary tube are 42°C, 110 mm and 1.7 mm respectively.

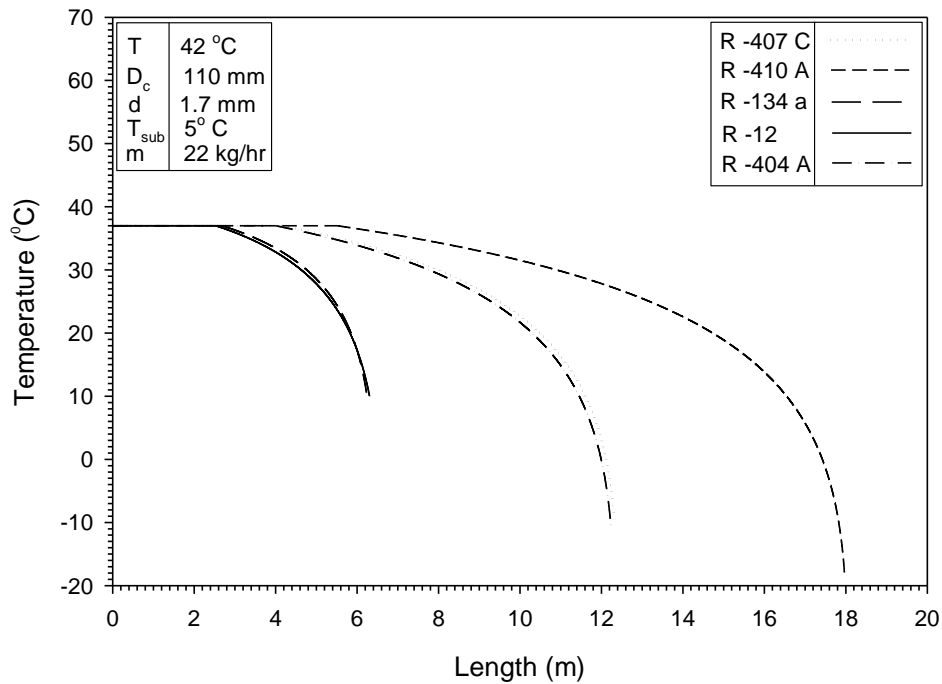


Fig.4.41: Variation of temperature for refrigerants R-407 C, R-410 A, R-134a, R-12 and R-404 A along a capillary tube length for temperature 42°C, 1.7 mm tube diameter, sub cooling 5°C and coil diameter 110 mm.

4.28 Different pressures of refrigerants R-407 C, R-410 A, R-134a, R-12 and R-404 A along a capillary tube length.

Fig.4.42 has been drawn for different pressure of different refrigerants for a single saturation temperature 42°C. All the refrigerant has different saturation pressures for single saturation temperature. Here in figure 4.42 different pressures of different refrigerants has been taken at single saturation temperature. A constant mass flow rate 28 kg/hr has been maintained for study. R-407 C and R-404 A follow almost the same path for pressure variation along the capillary length. R-134a and R-12 has the shortest span of length for the given pressure variation along the length. R-410 has the longest span of length for the given saturation pressure at temperature 42°C. Condenser temperature, coil diameter and diameter of capillary tube are 42°C, 110 mm and 1.7 mm respectively. All study values are taken at 5°C sub cooling.

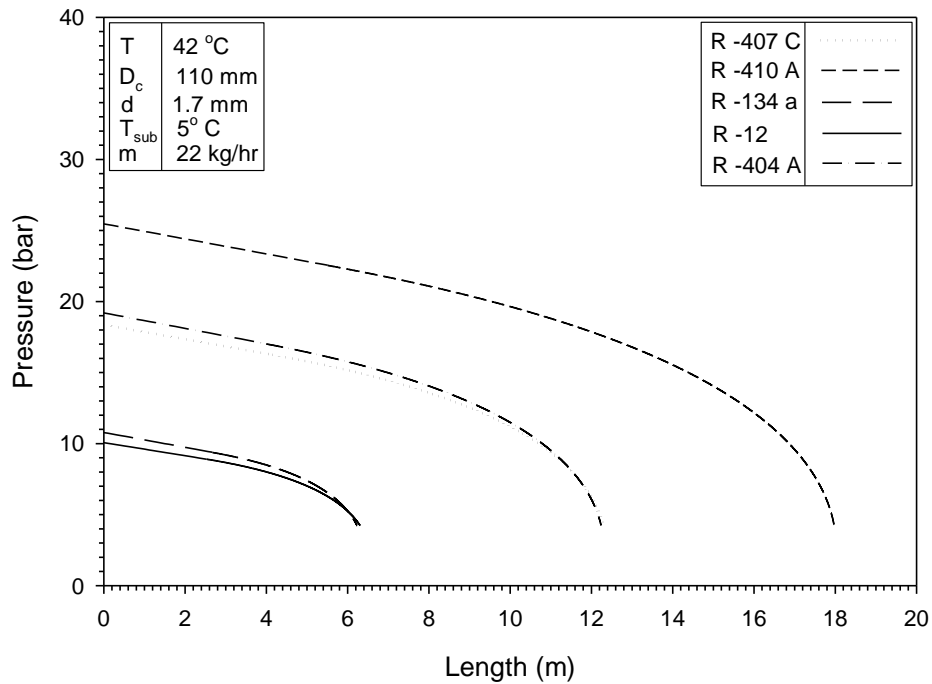


Fig.4.42: Different pressure variation for refrigerants R-407 C, R-410 A, R134a, R-12 and R-404 A along a capillary tube length for saturation temperature 42°C, 1.7 mm tube diameter, sub cooling 5°C and coil diameter 110 mm.

4.2.9 Different temperature of refrigerants R-407 C, R-410 A, R134a, R-12 and R-404 A along a capillary tube length.

Fig.4.43 has been drawn for different temperature of different refrigerants for a single saturation pressure 22 bar. All refrigerants have different saturation pressures for single saturation temperature. Here in figure 4.43 different temperatures of different refrigerants has been taken at single saturation pressure. A constant mass flow rate 28 kg/hr has been maintained for study. All refrigerant have constant temperature for single phase length and non linear variation for two phase length. R-407 C and R-404 A follow slightly different path for temperature variation along the capillary length. R-404 A has the shortest span of length for the given temperature drop along the length. R-12 has the longest span of length for the given saturation temperature at pressure 22 bar. Condenser pressure, coil diameter and diameter of capillary tube are 22 bar, 60 mm and 1.15 mm respectively. All study values are taken at 5°C sub cooling.

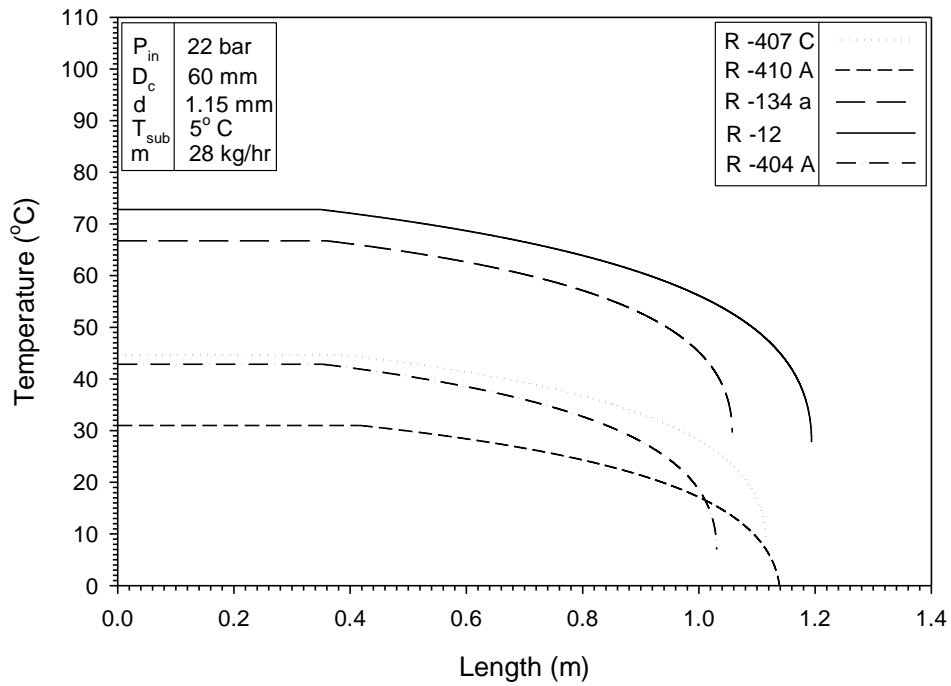


Fig.4.43: Different pressure variation for refrigerants R-407 C, R-410 A, R134a, R-12 and R-404 A along a capillary tube length for saturation pressure 22 bar, 1.15 mm tube diameter, sub cooling 5°C and coil diameter 60 mm.

Chapter - V

CONCLUSIONS AND FUTURE SCOPE OF WORK

5.1 CONCLUSIONS

The following conclusions are drawn from the present work:

- The numerical models for adiabatic helical capillary tubes have been developed. The proposed models can predict the capillary tube length for a given refrigerant mass flow rate as well as the refrigerant mass flow rate for a given capillary tube length.
- The proposed models for each capillary tube have been validated with the data of previous researchers.
- The proposed model for helical capillary has been validated with the experimental data of Kim *et al.* (2002), Mittal *et al.* (2009) and Khan *et al.* (2008).
- On an average M&N friction factor equation gives the best results for all the conditions.
- M&N+GIRI over predict the mass flow rate if compared to the available experimental data and it over predicts experimental data by 16%.
- C-M&N equation under predicts the mass flow rate by 10 %.
- It has been concluded that mass flow rate of refrigerants R-407 C, R-410 A, R-134a, R-12 and R-404 A increases with increase in degree of sub cooling.
- The proposed model results shows that coil diameter of adiabatic helical capillary tube affects mass flow rate of all refrigerants R-407 C, R-410 A, R-134a, R-12 and R-404 A to a little extent.
- The proposed model results show that mass flow rate decreases with increasing evaporator pressure.
- It also concludes that mass flow rate of refrigerants R-407 C, R-410 A, R-134a, R-12 and R-404 A increases tremendously with increase in capillary tube diameter.
- Mass flow rate of refrigerants R-407 C, R-410 A, R-134a, R-12 and R-404 A also increases with increase in capillary inlet pressure.

5.2 Scope of future work

Capillary tube has an advantage of its simple configuration over other type of complex expansion devices. It requires low starting torque and it brings the system in equilibrium automatically when power is off. Capillary tube is a small but an important component of any refrigerating or air-conditioning system. Conventional refrigerants have been phasing out with time due to their ozone depletion potential. As so many blends of refrigerants come into market for the replacement of the conventional refrigerants. So there can be more accurate mathematical model to size the capillary tube for different operating conditions of a refrigeration system. Another mathematical model with different friction factor and viscosity model can be developed for more accurate results. Simulation results can be tabulated for other non conventional refrigerants.

REFERENCES

- [1] Bansal P.K., Rupasinghe A.S. (1996), An empirical correlation for sizing capillary tubes, *Int.J. Refrigeration*. 19 (8), 497–505.
- [2] Choi J.M., Kim Y.C. (2002), The effects of improper refrigerant charge on the performance of heat pump with an electronic expansion valve and capillary tube. *Energy* 27 (4), 391–404.
- [3] C. Park, S. Lee, H. Kang, Y. Kim, Experimentation and modelling of refrigerant flow through coiled capillary tubes. *International Journal of Refrigeration* 30 (2007) 1168-1175.
- [4] C.Z. Wei, Y.T. Lin, C.C. Wang, A performance comparison between coiled and straight capillary tubes, *Heat Transfer Eng.* 21 (2) (2000) 62–66.
- [5] D.B. Jabaraj, A. Vettri Kathirvel, D. Mohan Lal (2006), Flow characteristics of HFC407C/HC600a/HC290 refrigerant mixture in adiabatic capillary tubes. *Applied Thermal Engineering* 26 (2006) 1621–1628.
- [6] Fiorelli, F.A.S., Huerta, A.A.S., Silvaes, O.M., 2002. Experimental analysis of refrigerant mixtures flow through adiabatic capillary tubes. *Exp. Therm. Fluid Sci.* 26, 499–512.
- [7] Guobing.Z and Yufeng.Z, (2006b), Experimental investigation on hysteresis effect of refrigerant flowing through a coiled adiabatic capillary tube. *Energy Conversion and Management*. 47 (2006) 3084-3093.
- [8] H. Ito, Laminar flow in curved pipes. *ZAMM Journal of Applied Mathematics and Mechanics* 11 (1969) 653-663.
- [9] Kuehl, S.J., Goldschmidt, V.W., 1990. Steady flows of R-22 through capillary tubes: test data. *ASHRAE Trans.* 96 (1), 719–728.
- [10] Khan, M.K., Kumar, R., Sahoo, P.K., 2008b. An experimental study of the flow of R-134a inside an adiabatic spirally coiled capillary tube. *Int. J. Refrigeration* 31 (6), 970–978.

- [11] Khan, M.K., Kumar, R., Sahoo, P.K., 2008a. Experimental study of the flow of R-134a through an adiabatic helically coiled capillary tube. HVAC&R Res. 14 (5), 749–762.
- [12] L. Yang, W. Wang, A generalized correlation for the characteristics of adiabatic capillary tubes. International Journal of Refrigeration 31 (2008) 197-203.
- [13] Li, R.Y., S. Lin and Z.H. Chen. 1990. Numerical modeling of thermodynamic non-equilibrium flow of refrigerant through capillary tubes, ASHRAE Trans., pp. 542 – 549.
- [14] M.K. Khan, R. Kumar, P.K. Sahoo, A homogeneous flow model for adiabatic helical capillary tube, ASHRAE Trans. 114 (1) (2008) 239–247.
- [15] Melo, C., Ferreira, R.T.S., Neto, C.B., Goncalves, J.M., Mezavila, M. M., 1999. An experimental analysis of adiabatic capillary tubes. Appl. Therm. Eng. 19 (6), 669–684.
- [16] M.K. Mittal, Ravi Kumar, Akhilesh Gupta, An experimental study of the flow of R-407 C in an adiabatic helical capillary tube. International journal of refrigeration 33 (2010) 840 – 847.
- [17] M.K. Mittal, Ravi Kumar , Akhilesh Gupta, Numerical analysis of adiabatic flow of refrigerants through a spiral capillary tube. International Journal of Thermal Sciences 48 (2009) 1348–1354.
- [18] M.K. Khan, R. Kumar, P.K. Sahoo, Flow characteristics of refrigerants flowing inside an adiabatic spiral capillary tube, HVAC&R Research ASHRAE 13 (2007) 731–748.
- [19] NIST. REFPROP 7.0, National Institute of Standards and Technology, Gaithersburg,MD, (1999).
- [20] O.Gercia-Valladares, Numerical simulation and experimental validation of coiled adiabatic capillary tubes. Applied Thermal Engineering 27 (2007) 1062–1071.
- [21] Sukkarin Chingulpitak, Somchai Wongwises, Effects of coil diameter and pitch on the flow characteristics of alternative refrigerants flowing through adiabatic helical capillary tubes. International Communications in Heat and Mass Transfer 37 (2010) 1305–1311.

- [22] Sukkarin Chingulpitak, Somchai Wongwises, Two-phase flow model of refrigerants flowing through helically coiled capillary tubes. *Applied Thermal Engineering* 30 (2010) 1927-1936.
- [23] Sukkarin Chingulpitak, Somchai Wongwises, A comparison of flow characteristics of refrigerant flowing through adiabatic straight and helical capillary tube. *International Communications in Heat and Mass Transfer* 38 (2011) 398–404.
- [24] S. Wongwises, P. Chan, N. Luesuwanatat, T. Purattanak, Two-phase separated flow model of refrigerants flowing through capillary tubes, *International Communications in Heat and Mass Transfer* 27 (3) (2000) 343–356.
- [25] S.M. Liang, T.N. Wong, Numerical modeling of two-phase refrigerant flow through adiabatic capillary tubes, *Applied Thermal Engineering* 21 (10) (2001) 1035–1048.
- [26] S.G. Kim, S.T. Ro, M.S. Kim, Experimental investigation of the performance of R-22, R-407C and R-410A in several capillary tubes for air-conditioners. *International Journal of Refrigeration* 25 (2002) 521-531.
- [27] T.N. Wong, K.T. Ooi, Adiabatic capillary tube expansion devices: a comparison of the homogeneous flow and the separated flow models, *Applied Thermal Engineering* 16 (7) (1996) 625–634.
- [28] Wei, C.Z., Lin, Y.T., Wang, C.C., Leu, J.S., 1999. An experimental study of the performance of capillary tubes for R-407C refrigerant. *ASHRAE Trans.* 105 (2), 634–638.
- [29] Wong T.N. and K.T. Ooi. 1996. Evaluation of capillary tube performance for CFC-12 and HFC-134a. *International communications in Heat and Mass Transfer*, vol. 23, pp.993-1001.
- [30] Zhou, G., Zhang, Y., 2006. Numerical and experimental investigations on the performance of coiled adiabatic capillary tube. *Appl. Therm. Eng.* 26, 1106–1114.